

POLITECNICO DI TORINO

MASTER'S DEGREE IN PHYSICS OF COMPLEX SYSTEMS



**Politecnico
di Torino**

MASTER'S DEGREE THESIS

Ecosystem stability and learning in linear quadratic network games

Candidate:
Adalberto Damino

Supervisor:
Prof. Luca Dall'Asta

October, 2023

Summary

In the context of Network Games, the linear quadratic model has been extensively used to model strategic interactions between a group of individuals or organisations. Due to its intrinsic simplicity, it allows to study games where a player's payoff not only depends on his own action but also on those of their neighbors, in an underlying network structure, with numerous potential applications in economics and social sciences. When all players have full and perfect knowledge of the game, including the rules, possible strategies, payoffs, and the actions taken by other players, the analysis of Nash equilibria can be done by studying the topological properties of the network (1). However, in more realistic scenario, it is common to observe uncertainty on both the network structure and game properties, leading to the study of a generalized game where a player lacks information on who he's interacting with, and the strength of his externalities. The best response is then based on a subjective beliefs: we imagine that an agent is unaware of the identity of her neighbors and she receives only an aggregate contribution she best responds to in order to maximize her utility. The learning process leads to conjectural best response paths that may possibly converge to a steady state, which represents a generalization of the equilibrium state, called Self-Confirming Equilibrium (SCE) (2). When only local externalities are present, the SCE set can be characterized by means of the Nash equilibrium of the auxiliary game with complete information where only active agents are present, this is related to the fact that if an agent becomes inactive after a certain time period of the learning dynamics, it will remain inactive for the rest of the game. As a consequence, the outcome of the learning process will result in a portion of the community that will reach an inactive absorbing state, while the rest will, possibly, converge to a steady state. A similar scenario can be observed in the study of the generalized Lotka-Volterra equations, which are frequently used to describe the dynamics of predator-prey interactions in ecology. Similarly to the linear quadratic model, one must analyze the dynamics of N interacting degrees of freedom, which is in principle deterministic once the initial conditions and network topology are fixed. To focus on typical properties of the community, the ecosystem can be treated as the outcome of a random choice, within a statistical ensemble of possible network structures: random Lotka-Volterra equations can then be recasted into a 1 body self-consistent stochastic dynamics through a dynamical mean field theory approach in the thermodynamical limit (3), averaging over all possible sources of uncertainty. In ecology, one finds a region in which one competitive equilibrium exists and one region in which the total biomass in the system explodes as a consequence of unbalanced interactions. In this work the linear quadratic model is analysed with the same approach, focusing on the role of anticorrelated and mutualistic interactions, stability and connectivity of the network. Similarly to the case of ecological communities, it is shown that under some conditions on the structure of the network, the learning process can lead to inactivity traps, in which a, possibly large, fraction of the network does not contribute to the system. Non-cooperative interactions surprisingly promote stability, while also favouring an increasing fraction of surviving agents at the steady state. Connectivity plays a crucial role in the outcomes of the learning process, promoting as well the stability of the community.

Contents

Summary	iii
1 Introduction to the models	1
1.1 Generalized Lotka Volterra Equations	1
1.1.1 Introduction to the L-V two species model	1
1.1.2 Generalized Lotka Volterra	2
1.2 Linear Quadratic Network Games	3
1.2.1 Game with complete information	4
1.2.2 Game with incomplete information	6
1.2.3 Conjectural best-reply learning paths	7
2 Dynamical mean field theory	9
2.1 Introduction to DMFT	9
2.2 Random Lotka-Volterra systems	10
2.2.1 Generating functional approach	10
2.2.2 The representative process	14
2.2.3 Fixed points analysis	14
2.2.4 Numerical procedure	16
2.2.5 Order parameters	17
2.2.6 Linear stability of steady states	18
2.2.7 Results of the model	20
2.2.8 Cavity Method	21
2.3 Linear quadratic systems	24
2.3.1 Generating Functional approach	25
2.3.2 The representative process	29
2.3.3 The stationary state (at fixed α)	30
2.3.4 Numerical procedure	31
2.3.5 Stability analysis of the stationary state	31
3 Comparison with simulations	35
3.1 Introduction to the method	35
3.2 Case of complete graph	37
3.2.1 Interpretation of the results	39
3.2.2 Effect of divergence and instability	39
3.3 Case of K regular random graph	43
4 Conclusions	45

Chapter 1

Introduction to the models

1.1 Generalized Lotka Volterra Equations

1.1.1 Introduction to the L-V two species model

Lotka Volterra equations provide a simple tool for understanding how the populations of species might change over time in response to each other's interactions. In the simplest case, the equations account for the evolution of two interacting species. The model was developed independently during the 1920s by American mathematician and physical scientist Alfred J. Lotka and Italian physicist Vito Volterra. The equations take the form:

$$\begin{aligned}\frac{dx_1(t)}{dt} &= r_1 x_1(t) [K_1 - x_1(t) + z_{12} x_2(t)] \\ \frac{dx_2(t)}{dt} &= r_2 x_2(t) [K_2 - x_2(t) + z_{21} x_1(t)]\end{aligned}\tag{1.1}$$

Where:

- $x_i(t)$ is the population density of species i at time t , with initial conditions $x_i(t=0)$
- r_i is the basal growth rate of species i
- K_i is the carrying capacity of species i
- z_{ij} is the interaction strength from i to j , that is to say the strength of the effect that species j has on the dynamics of species i

In absence of interactions, assuming initial conditions smaller than the carrying capacities, the density of the two species will exponentially increase in time until they will saturate to the asymptotic values K_1 and K_2 according to the logistic growth. On the other hand, interaction introduces a lot of variety in the outcomes of the dynamics. The existence of an equilibrium point will depend on the initial conditions for densities $x_i(t)$, parameters r_i and K_i and the sign and absolute value of interaction strengths z_{ij} and z_{ji} , that can be seen as entries of an interaction matrix \mathbf{Z} . Interaction represents the type and strength of the relation between the two species: a competitive interaction occurs when both z_{ij} and z_{ji} are negative (such as competition between shared common resources), predator prey interaction when $z_{ij} > 0$ and $z_{ji} < 0$, in which case species i and j will be respectively the prey and the predator, or mutualistic interactions when both parameters are positive. Once the initial conditions and parameters of the model are fixed, the outcome will be deterministic. In general, we can find four possible scenarios: either species can

be the sole survivor, one species is always the sole survivor (competitive exclusion), or the two species can reach a coexistent equilibrium state, whose stability depends again on the parameters of the model.

1.1.2 Generalized Lotka Volterra

The Generalized Lotka Volterra equations (GLV) model the dynamics of ecological communities made of an arbitrary number of interacting species.

$$\frac{dx_i(t)}{dt} = r_i x_i(t) \left[K_i - x_i(t) + \sum_{j \in \partial_i} z_{ij} x_j(t) \right] \quad (1.2)$$

For $i = 1 \dots N$.

Now species i can be imagined as a node inside a network $G = (I, \mathbf{Z})$ that interacts with his out-neighbourhood ∂_i through interaction coefficients z_{ij} . In some applications, a small immigration rate λ_i is added to model situations of new individuals arriving to the ecosystem from the outside. Similarly to the two species model, once initial conditions and parameters are fixed, the equations are deterministic and can possibly converge to a stationary solution whose stability will depend on the topological properties and parameters of the network, especially on the spectral properties of the interaction matrix \mathbf{Z} . The analysis of global stability is in general difficult to approach, as an alternative, one can test for local asymptotic stability, that is to ask whether the system will return to the equilibrium if perturbed infinitesimally, or move away from it. An alternative approach would be to focus on random communities, where the structural parameters of the model, as well as initial conditions, follow a specific probability distribution. In order to study the stability of large random communities, the results obtained in Random Matrix theory have shown to be very useful (4). The analysis of dynamical systems with random parameters also allows one to derive interesting results that are meant to describe the “typical” or “expected” community rather than a particular realization of the network, by working with a statistical ensemble of graphs in the thermodynamical limit $N \rightarrow \infty$. One of the main advantages is that the obtained results can be associated to topological properties of the graph, such as connectivity or centrality. This approach also allows to account for interaction types, since in ecological communities the effect of species i on j and viceversa are usually not independent: in the case of competition we expect both coefficients to be negative, while for the predator prey case we expect them to have opposite sign, and so forth. A more refined model for the interaction matrix would therefore sample interactions in pairs, from a bivariate distribution with components (z_{ij}, z_{ji}) . A convenient choice would be to draw the couplings z_{ij} ($i \neq j$) from a gaussian bivariate distribution defined by its mean μ and covariance matrix, this introduces a model parameter controlling the correlation between the interaction coefficients z_{ij} and z_{ji} , and hence the fraction of prey predator pairs in the artificial ecological system. For any $i < j$ we have

$$z_{ij} = \frac{\mu}{N} + \frac{\sigma}{\sqrt{N}} w_{ij} \quad z_{ji} = \frac{\mu}{N} + \frac{\sigma}{\sqrt{N}} w_{ji} \quad (1.3)$$

Where w_{ij} and w_{ji} are drawn from a Gaussian distribution with $\overline{w_{ij}} = 0$ and covariance matrix

$$\Sigma = \begin{pmatrix} 1 & \gamma \\ \gamma & 1 \end{pmatrix} \quad (1.4)$$

The scaling of the moments of the z_{ij} with N is necessary to produce a well defined limit $N \rightarrow \infty$ in which the statistical mechanics theory applies. The parameter $-1 \leq \gamma \leq 1$ describes the correlations between w_{ij} and w_{ji} , i.e. $\overline{w_{ij}w_{ji}} = \gamma$. For $\gamma = 1$ one has $w_{ij} = w_{ji}$, and as a consequence $z_{ij} = z_{ji}$, with probability one. For $\gamma = 0$, w_{ij} and w_{ji} are uncorrelated, and for $\gamma = -1$ one has $w_{ij} = -w_{ji}$ with probability one. In the limit of large system size, a given pair of species $i \neq j$ forms a predator prey pair ($z_{ij}z_{ji} < 0$) if and only if w_{ij} and w_{ji} are of opposite sign. The percentage p of predator prey interactions in the network can then be computed by performing a suitable Gaussian integral over the joint distribution of w_{ij} and w_{ji} . This leads to an explicit, non linear and decreasing dependence of p on γ . In particular one has $p = 1$ for $\gamma = -1$ (for $\gamma = -1$ the system consists fully of predator prey interactions); one has $p = 1/2$ for $\gamma = 0$ (50% predator prey pairs), and $p = 0$ for $\gamma = 1$ (i.e., no prey predator pairs are present for $\gamma = 1$). In all cases, the remaining fraction of $1 - p$ interaction pairs is not of the predator prey type. In the limit $N \rightarrow \infty$, half of these will be of a mutualistic interaction type (z_{ij} and z_{ji} both positive), and the other half of a strictly competitive type (z_{ij} and z_{ji} both negative). This approach allows to investigate the role of predator prey pairs in the properties, such as stability, of this artificial ecosystem. In order to analyze fixed-point properties and statistics of the random ecological community at stationarity one can use dynamical methods from spin-glass physics (5), in the limit $N \rightarrow \infty$, that will be discussed in chapter 2.

1.2 Linear Quadratic Network Games

The interaction of multiple independent decision-makers can be modelled inside a network, where each agent represents a node inside a graph interacting through links. It has a wide range of applications in contexts where individuals or groups interact with one another, and an individual's payoff depends not only on their action but also on those of her neighbors. The topological properties of the networks play a crucial role in determining the behaviour and actions of the players. The analysis of existence and unicity of Nash equilibria for a system of N interacting degrees of freedom is, in general, not an easy task to tackle. It is convenient to consider games simple enough to be studied, while still being able to represent the outcomes of a game due to interaction. That's why the linear quadratic (LQ) model represents a broad class of games that have been extensively studied in the literature. The utility function for player i has the following form:

$$u_i(a_i, a_{-i}) = \alpha_i a_i - \frac{1}{2} a_i^2 + a_i \sum_{j \in \partial_i} z_{ij} a_j \quad (1.5)$$

With $G = (I, \mathbf{Z})$; $i, j \in I$.

Where I is the set of players ($|I| = N$), and $a_i \in A_i = [0, \infty[\in \mathbf{R} \forall i \in I$. The utility of player i not only depends on her action $a_i \geq 0$ but also those of the other players a_{-i} , specifically of her neighbors. The first term is a linear contribution in the action of player i weighted by the real coefficient $\alpha_i > 0$, which represents the

individual pleasure of agent i from being active on the network in isolation. The second term, quadratic in a_i , yields a linear best response. The third term captures interaction: $z_{ij} \in \mathbf{Z}$ is the intensity and the type (sign) of externality from j to i , it can be seen as an entry to the weighted adjacency matrix \mathbf{Z} of the network. If $z_{ij} \neq 0$ then j is a peer of i , i.e. the activity of j influences the utility of i . The last term will be referred in the following as the term of local externalities. In some applications, in addition to local externalities, a global term of the form $\gamma a_i \sum_{j \in I} a_j$ might be added, to model situations where players experience global competitive effects. The linear quadratic form of the payoff function in equation (1.5) allows for an easy characterization of equilibrium as a function of the network. It has been widely used to model competitive scenarios with relevant features of the strategic interactions, such as games of strategic complements and strategic substitutes. In games of strategic complements, an increase in the actions of other players leads a given player's higher actions to have relatively higher payoffs compared to that player's lower actions. That would be the case of students working together into a joint assignment or firms working on a collaborative research project. In games of strategic substitutes, however, the situation is opposite, such as the case of firms competing on market prices or individuals on local public goods. Also it can be used as a toy model to approximate games with complex non-linear payoffs. Some applications of the quadratic model are the analysis of crime activity, education outcomes, and competition between firms (2). In some particular cases it is possible to find an explicit solution for equilibrium behavior as a function of the network properties (1).

1.2.1 Game with complete information

When all players share common knowledge of the network structure, action sets, couplings and utility functions it is possible to characterize the set of Nash equilibria and to study its stability properties. In games of strategic complements and strategic substitutes, one can exploit some natural and useful monotonicity properties of the interaction in payoffs between players. We can look as example to the case where interaction occurs on a graph with unweighted adjacency matrix W , with a unique constant coupling parameter β among all players that are connected through an edge.

$$u_i(a_i, a_{-i}) = \alpha_i a_i - \frac{1}{2} a_i^2 + \beta a_i \sum_{j \in \partial_i} W_{ij} a_j \quad (1.6)$$

The sign of β determines the type of strategic interactions: β can either be positive or negative, and it represents respectively a case of strategic complements and substitutes. In this case $\mathbf{Z} = \beta W$. It has been shown that, assuming that the spectral radius of the matrix βW , denoted by $\rho(\beta W)$, is less than 1, there exists a unique interior Nash equilibrium with the following matrix from:

$$\mathbf{a} = (\mathbf{I} - \beta \mathbf{W})^{-1} \underline{\alpha} \quad (1.7)$$

Where $\underline{\alpha} = \alpha_i \mathbf{1}$ with $\mathbf{1}$ being an N -dimensional column vector of ones and \mathbf{I} the identity matrix. The equilibrium state in equation (1.7) can be rewritten as $\mathbf{a} = \sum_{p=0}^{\infty} \beta^p \mathbf{W}^p \underline{\alpha}$ which shows that, if $\underline{\alpha}$ is a vector of all ones, then each entry of \mathbf{a} is the Katz-Bonacich centrality of the corresponding agent, that is to say the number

of walks of any length p originated from that node discounted exponentially by β . This shows that despite the presence of only local externalities in equation (1.5) the payoff interdependency actually spreads indirectly throughout the network, and that the Nash equilibrium action state of a player is strictly connected (that is, proportional) to her Bonacich centrality inside the graph, thus establishing a bridge with the sociology literature on social networks. It was also shown that a denser and larger network of local interactions increases the aggregate equilibrium outcome, roughly because both the number of paths and their weights increases with an increase in network connectivity and size (1).

1.2.2 Game with incomplete information

The current literature has largely focused on analyzing the characteristics of network games where the structure of the network is known beforehand. In more realistic scenarios, however, while the actions of the players may be observable, the underlying interaction network remains hidden. Agents may ignore how the network affects their payoffs, how the network is shaped, or even that they are interacting in a network. This raises the question of when and why we might expect that observed play in a game will correspond to one of the Nash equilibria. An alternative explanation is that equilibrium arises as the long run outcome of a process in which less than fully rational players grope for optimality over time. Learning models can thus suggest useful ways to evaluate and modify traditional equilibrium concepts, leading to refinements of Nash equilibrium, while still being consistent with the latter, hence Nash equilibrium action profiles will be limit outcomes of learning paths where agents have perfect feedback about the payoff relevant aspects of others' behavior, while with imperfect feedback non-Nash action profiles may result as the steady state limits of learning paths. A variety of learning models have been proposed, with different motivations, and they differ widely in terms of what prompts players to make decisions and how sophisticated players are assumed to be. In the simplest models, players behave by using strategies that have worked in the past. In other models, players explicitly maximize payoffs given beliefs, these beliefs may involve varying levels of sophistication. We'll use the latter approach to model a learning process for the game shown in equation (1.5), following the work of Battigalli P. et al in (6).

As already discussed, uncertainty about the game introduces the need for refinements of Nash equilibrium. Depending on the source of uncertainty, an agent could learn by best responding to subjective beliefs about the payoff relevant aspects of what others are doing, such as their play, and that may or may not be correct, with the possibility for beliefs to be confirmed by the observed outcome while being incorrect about off-path play. As a result, the learning process can converge to outcomes that cannot be generated by any Nash equilibrium of the game. For this reason, notions of "subjective" equilibrium have been developed in the context of repeated games: in a Self-Confirming Equilibrium (SCE) each player's strategy is optimal given his beliefs about the opponents' strategies, but each player's beliefs are correct only at the information sets that are reached in her play. While for a Nash, each player's beliefs are correct at every information set (2). The notion of SCE will be crucial in the analysis of our learning process.

1.2.3 Conjectural best-reply learning paths

The learning process will be structured as follows: an agent i will be unaware of the identity of her neighbors, receiving only an aggregate contribution she best responds to in order to maximize her utility for the next iteration of the game, while she will know that her optimal action depends on an unknown state, also referred in the following as payoff state, that is, actually, an aggregate of the actions of her neighbors. The corresponding sequence of action profiles $(\mathbf{a}_t)_{t=0}^{\infty}$ forms a conjectural best-reply path. An agent i doesn't know neither who's interacting with nor what type of influence their specific play have on her utility. In light of this, we rewrite eq (1.5) as:

$$v_i(a_i, b_i) = \alpha_i a_i - \frac{1}{2} a_i^2 + a_i b_i \quad (1.8)$$

Where now v_i is the realized payoff observed by player i , and b_i is the payoff state, i.e. the realized value of the aggregate contribution of the term $\sum_{j \in \partial_i} z_{ij} a_j$. Agent i knows α_i , the form of her utility and how it depends on his action, which will be chosen in a bounded interval $a_i \in [0, \bar{a}_i] = A_i$, as consequence the payoff state will be bounded $b_i \in [\underline{b}_i, \bar{b}_i] = B_i$. Starting from a set of initial conditions $\{a_i(0)\}_{i=1..N}$, an agent receives $v_i(t=0)$ as feedback, conjectures the value of the payoff state \hat{b}_i and best responds to it by choosing an action that maximizes her utility, and that will be valid for the next time step. This update will be simultaneous for all players. From the form of v_i we notice that the feedback received by players is such that, if an agent i decides to be inactive ($a_i = 0$), then she cannot learn anything about the game and about what others are doing (the realized value of b_i), thus she cannot observe whether inactivity was a best reply to peers' activity. If she finds it subjectively optimal to be inactive, such lack of information about the payoff state creates an "inactivity trap", allowing her possibly wrong conjecture to persist. If we imagine a_i to be an activity level for the agent, this framework mimics situations where agents are likely to ignore relevant information if they opt out from the network, while active players have a quasi-perfect feedback about what happens, being able to deduct the payoff state.

$$b_i = \frac{v_i - \alpha_i a_i + \frac{1}{2} a_i^2}{a_i} = \frac{v_i}{a_i} - \alpha_i + \frac{1}{2} a_i$$

If an agent experiences a negative payoff because some of her neighbors whose externalities toward her are negative played high actions (hence, giving negative feedback), then she may choose to abstain from interacting. Later, game conditions may improve, making it objectively profitable to be active, but the now inactive agent cannot observe it, thus remaining in an inactive absorbing state. Agents update their beliefs in response to the feedback they receive, which is assumed to be their payoff, and maximize their instantaneous expected payoff given such updated beliefs. This updating process yields learning paths that do not necessarily converge to a Nash equilibrium of the game. Nevertheless, in equilibrium, an agent conjecture must be consistent with the feedback received, that is, confirmed. The best reply function for player i has the following form:

$$BR_i(b_i) = \begin{cases} 0, & b_i \leq -\alpha_i \\ \alpha_i + b_i & -\alpha_i \leq b_i \leq \bar{a}_i - \alpha_i \\ \bar{a}_i & b_i \geq \bar{a}_i - \alpha_i \end{cases}$$

Since $\alpha_i > 0$, we may have $BR_i(b_i) = 0$ only if $b_i < 0$.

A profile $(a_i^*, b_i^*) \in \prod_{i \in I} (A_i \times B_i)$ of actions and deterministic conjectures is a Self Confirming Equilibrium at \mathbf{Z} if, for each $i \in I$

1. (Subjective rationality) $a_i^* = BR_i(\hat{b}_i)$
2. (Confirmed conjecture) $v_i(a_i^*, \hat{b}_i) = v_i(a_i^*, b_i)$

Condition 1 requires that each agent best responds to her subjective belief about the payoff state, while condition 2 requires that the expected payoff is equal to the realized payoff. Notice that the latter condition do not imply conjectures to be correct. One can draw a correspondence between the set of actions profiles that are Self Confirming Equilibria \mathbf{N}_Z^{SCE} , and the set of (pure) Nash action profiles \mathbf{N}_Z^{NE} , for a given game described by interaction matrix \mathbf{Z} . First we can notice that any Nash equilibrium \mathbf{a}^* corresponds to a Self Confirming Equilibrium with correct conjectures, from which we can deduce $\mathbf{N}_Z^{NE} \subseteq \mathbf{N}_Z^{SCE}$. Within our learning process, inactivity traps are deeply related to the structure of the SCE set, since the only way to observe in the steady states conjectures that are confirmed but not correct is given by the possibility for an agent i to enter an absorbing state $a_i = 0$. If being inactive is dominated, for example when local externalities are positive and this is known, then Nash and Self Confirming equilibrium action profiles coincide. However, if there are agents for whom being inactive is not dominated, for example when some negative local externalities are present, then any subset of this set of agents may be inactive in some Self Confirming equilibrium. In this case inactivity is a best reply to confirmed, but possibly false conjectures. Since, for each \mathbf{Z} , the joint best-reply function is a continuous self-map on the compact and convex subset $\prod_{i \in I} A_i \subset \mathbb{R}^I$ Brouwer Fixed Point Theorem implies that a Nash equilibrium, and as a consequence a Self Confirming equilibrium, exists for each game given \mathbf{Z} .

Let I_0 be the set of players for whom being inactive is justifiable, that is

$$I_0 := \{i \in I : \exists b_i \in B_i, BR_i(b_i) = 0\} = \{i \in I : \alpha_i + \underline{b}_i \leq 0\}$$

Also, for each interaction matrix \mathbf{Z} and non-empty subset of players $J \subseteq I$, let $\mathbf{A}_{J,Z}^{NE}$ be the set of Nash equilibria of an auxiliary game where only the subset J of agents is considered. Then, for each \mathbf{Z} the set of Self Confirming action profiles is

$$\mathbf{A}_Z^{SCE} = \bigcup_{J: I \setminus J \subseteq I_0} \mathbf{A}_{J,Z}^{NE} \times \mathbf{0}_{I \setminus J}$$

In every possible SCE action profile there will be subset (possibly null) of inactive agents, for whom being inactive is undominated, while the rest will converge to a (possibly unique) Nash Equilibrium of the auxiliary game where only active players are present. If being inactive is unjustifiable for every agent then the SCE coincides with NE set. Notice that I_0 and J are not necessarily disjoint sets. Thus, the SCE set can be characterized by means of the Nash equilibria of the auxiliary games in which only active agents are considered. For example, in the game given in eq (1.6), for $\beta > 0$ where all local externalities are positive and this is common knowledge, the two equilibrium sets coincide. For the game in eq (1.8), assuming certain properties of the matrix \mathbf{Z} , one can also provide sufficient conditions to have arbitrary sets of inactive and active players in a Self Confirming Equilibrium, as shown in (6).

Chapter 2

Dynamical mean field theory

2.1 Introduction to DMFT

Both models that were introduced involve systems of heterogeneous agents that interact in cooperative and competitive manner, leading to a rich and complex dynamics. We are dealing with disordered systems, that is, systems whose structural parameters are themselves the outcome of a random choice. Rather than focusing on the analysis of a system where the network structure is fixed, it is possible to describe the large scale competitive behaviours, by developing a theoretical framework whose purpose is to grasp the typical features of the community, and to consider the full dynamics of these out-of-equilibrium systems. The typically large size of these systems opens the possibility of exploiting the thermodynamical limit $N \rightarrow \infty$ to obtain a tractable theory, with the prospect of obtaining universal results. Dynamical mean field theory (DMFT) is a theoretical approach to disordered statistical models that describes the time evolution of a typical degree of freedom after the average over the quenched disorder has been carried out, and yields a closed description of the dynamics in terms of an effective species and a small number of order parameters. Where "quenched" describes a disordered state that is not in thermodynamic equilibrium. DMFT method was first introduced to describe the dynamics of spin glasses (5), it also proved to be successful in describing phase transitions in other areas, such as neural networks and ecosystems. For the latter, the generalized Lotka-Volterra model is taken as a starting point, the theory has revealed that dynamical models for ecosystems can exist in a variety of phases, characterized either by a single equilibrium, multiple marginally-stable equilibria, or chaos. The main ingredients to construct a dynamical mean field theory are the following. Consider a generic theory with dynamical variables $x_i(t)$ with $i = 1, \dots, N$ in the presence of disorder. Depending on the context, these could be spin variables, or species abundances, for which disorder is introduced via random coupling coefficients, or random inter-species interactions. In a Dynamical mean field theory, one usually finds a Langevin dynamics for the variables $x_i(t)$, either by path-integral methods (3), or the dynamical cavity methods (7), by performing a disorder average. The many-species dynamical problem is then reduced to an effective process for a representative degree of freedom: from a set of N coupled differential equations we find a 1-body stochastic dynamics x^* , that captures the statistics of the community, following self-consistent equations. A consequence of the disorder average is however to introduce time quantities and time correlation effects. The most basic of these are the correlation function $C(t, t') = \frac{1}{N} \sum_i \langle x_i(t)x_i(t') \rangle$, where $\langle (\dots) \rangle$ denotes the average over disorder subject to appropriate initial conditions. Also a response function $R(t, t') = \frac{1}{N} \sum_i \langle \frac{\delta x_i(t)}{\delta h_i(t')} |_{h=0} \rangle$, here $h_i(t)$ is a field conjugate to the dynamical variable $x_i(t)$. In the simplest class of DMFTs, one obtains a pair

of integro-differential equations involving $C(t, t')$ and $R(t, t')$. In the following, the DMFT approach is applied both to the GLV and LQ models via a generating functional approach, with the purpose to draw a meaningful correspondence between the obtained results. Finally, the same results will be obtained via the cavity method, in order to gain more of a physical insight on this approach.

2.2 Random Lotka-Volterra systems

We start from GLV equations 1.2, setting $r_i = K_i = 1$.

$$\frac{dx_i(t)}{dt} = x_i(t) \left[1 - x_i(t) + \sum_{j \in \partial_i} z_{ij} x_j(t) \right] \quad (2.1)$$

For $i = 1 \dots N$.

We'll assume that the elements of the interaction matrix (z_{ij}, z_{ji}) follow a bivariate gaussian distribution given by (1.3) and (1.4). $x_i(t) \geq 0$ is the population density of species i at time t . The initial conditions $x_1(0), \dots, x_N(0)$ can also be random, that is, drawn from some joint probability distribution. Scalar functions of time will be denoted by underlined symbols, e.g. $\underline{x} = (x(t=0), x(t=1), \dots, x(t=T))$, while general column vectors by bold face letters, such as $\mathbf{x} = (x_1, \dots, x_N)^T$. Once initial conditions and interaction parameters are fixed, the GLV dynamics contains no further randomness during the time evolution.

2.2.1 Generating functional approach

First, we write a dynamical generating functional for the process, which is defined as:

$$Z[\underline{\Psi}] = \int D\underline{\xi} D\underline{x} p(\underline{\xi}) \delta(\text{equations of motion}) e^{i \sum_i \int dt x_i(t) \Psi_i(t)}$$

Where $\underline{\xi}$ is the source of stochasticity for the dynamical process $x_i(t)$. In our case it will be the interaction parameters z_{ij} , assuming initial conditions are fixed. Once parameters are drawn, $x_i(t)$ is constrained to paths of the dynamics of the Lotka-Volterra equations through a delta function. Also, it can be seen as:

$$Z[\underline{\Psi}] = \left\langle e^{\underline{x} \cdot \underline{\Psi}} \right\rangle$$

Where $\underline{x} = \{x_i(t)\}_{i,t}$ is a random vector, continuous in time, while $\langle (\dots) \rangle$ denotes the average over disorder. We now proceed with various manipulations in the generating functional. Expressing the delta function as its Fourier transform, and keeping at first the network parameters as fixed, we have:

$$Z[\underline{\Psi}] = \int D[\underline{x}, \underline{\hat{x}}] \exp \left\{ i \sum_i \int dt \hat{x}_i(t) \left[\frac{\dot{x}_i(t)}{x_i(t)} - \left(1 - x_i(t) + \sum_{i \neq j} z_{ij} x_j(t) + h(t) \right) \right] \right\} \\ \times \exp \left\{ i \sum_i \int dt x_i(t) \Psi_i(t) \right\}$$

Where we denoted $D[\underline{x}, \hat{\underline{x}}] = D_{\underline{x}} D_{\hat{\underline{x}}}$.

A time dependent field $h(t')$ is introduced in the equation of motion. This is needed to describe how the density $x_j(t)$ 'typically' reacts to perturbations at time t' by looking at the response function. Now, let us introduce some macroscopic order parameters:

$$\begin{aligned} M(t) &= \frac{1}{N} \sum_i x_i(t) \\ P(t) &= \frac{i}{N} \sum_i \hat{x}_i(t) \\ C(t, t') &= \frac{1}{N} \sum_i x_i(t) x_i(t') \\ K(t, t') &= \frac{1}{N} \sum_i x_i(t) \hat{x}_i(t') \\ L(t, t') &= \frac{1}{N} \sum_i \hat{x}_i(t) \hat{x}_i(t') \end{aligned}$$

Next, we isolate the term X containing the disorder (the $\{z_{ij}\}_{i \neq j}$):

$$X = \doteq \exp \left\{ -i \sum_{i \neq j} \int dt \hat{x}_i(t) z_{ij} x_j(t) \right\}$$

and perform the Gaussian average, exploiting eqs (1.3) and (1.4). The final form of the disorder term can be expressed in terms of the macroscopic parameters described above:

$$\begin{aligned} \langle X \rangle &= \left\langle \exp \left\{ -i \sum_{i \neq j} \int dt \hat{x}_i(t) z_{ij} x_j(t) \right\} \right\rangle \\ &= \exp \left\{ -\mu N \int dt P(t) M(t) \right. \\ &\quad \left. - \frac{1}{2} N \sigma^2 \int dt dt' [L(t, t') C(t, t') + \gamma K(t, t') K(t', t)] + \mathcal{O}(N^0) \right\} \end{aligned}$$

The notation $\mathcal{O}(N^0)$ indicates that we have left out sub-leading contributions in N (i.e, terms of order N_0 or lower). This includes for example terms such as $-i \frac{\mu}{N} \sum_i \int dt \hat{x}_i(t) x_i(t)$

We do this because we are eventually going to take the limit $N \rightarrow \infty$ after which these terms do not contribute.

These order parameters can formally be introduced into the generating functional as delta-functions in their exponential representation, e.g:

$$\begin{aligned} 1 &= \int \prod_{t, t'} dC(t, t') \delta \left(C(t, t') - \frac{1}{N} \sum_i x_i(t) x_i(t') \right) \\ &= \int D\underline{C} D\underline{\hat{C}} \exp \left\{ iN \int dt dt' \hat{C}(t, t') \left(C(t, t') - \frac{1}{N} \sum_i x_i(t) x_i(t') \right) \right\} \end{aligned}$$

and similarly for the other order parameters. We have chosen the scaling of the conjugate parameter $\hat{C}(t, t')$ such that the overall exponent contains a prefactor N .

The disorder-averaged generating functional can be written as follows:

$$\int D[\underline{M}, \underline{C}, \underline{L}, \underline{K}, \underline{P}, \underline{\hat{M}}, \underline{\hat{C}}, \underline{\hat{L}}, \underline{\hat{K}}, \underline{\hat{P}}] \exp \left\{ N \left[\Psi + \Phi + \Omega + \mathcal{O}(N^{-1}) \right] \right\} \quad (2.2)$$

The term:

$$\begin{aligned} \Psi = & i \int dt \left[\hat{M}(t)M(t) + \hat{P}(t)P(t) \right] \\ & + i \int dt dt' \left[\hat{C}(t, t')C(t, t') + \hat{K}(t, t')K(t, t') + \hat{L}(t, t')L(t, t') \right] \end{aligned}$$

results from the introduction of the macroscopic order parameters. The contribution

$$\begin{aligned} \Phi = & -\frac{1}{2}\sigma^2 \int dt dt' \left[L(t, t')C(t, t') + \gamma K(t, t')K(t', t) \right] \\ & - \mu \int dt M(t)P(t) \end{aligned}$$

comes from the disorder average, while Ω describes the details of the microscopic time evolution

$$\begin{aligned} \Omega = & N^{-1} \sum_i \log \left[\int D[x_i, \hat{x}_i] p_0^{(i)}(x_i(0)) \exp \left\{ i \int dt \psi_i(t) x_i(t) \right\} \right. \\ & \times \exp \left\{ i \int dt \hat{x}_i(t) \left[\frac{\dot{x}_i(t)}{x_i(t)} - \left(1 - x_i(t) \right) - h(t) \right] \right\} \\ & \times \exp \left\{ -i \int dt dt' \left(\hat{C}(t, t') x_i(t) x_i(t') + \hat{L}(t, t') \hat{x}_i(t) \hat{x}_i(t') + \hat{K}(t, t') x_i(t) \hat{x}_i(t') \right) \right\} \\ & \left. \times \exp \left\{ -i \int dt \left(\hat{M}(t) x_i(t) + i \hat{P}(t) \hat{x}_i(t) \right) \right\} \right] \end{aligned} \quad (2.3)$$

The quantity $p_0^i(\cdot)$ describes the distribution from which the initial values of the $\{x_i\}_{i=1..N}$ are drawn. We next use the saddle-point method to carry out the integral in Eq. (2.2). This is valid in the limit $N \rightarrow \infty$, and amounts to finding the extrema of the term in the exponent. Setting the variation with respect to the integration variables M, P, C, K and L to zero gives

$$\begin{aligned} i\hat{M}(t) &= \mu P(t) \\ i\hat{P}(t) &= \mu M(t) \\ i\hat{C}(t, t') &= \frac{\sigma^2}{2} L(t, t') \\ i\hat{K}(t, t') &= \gamma \sigma^2 K(t, t') \\ i\hat{L}(t, t') &= \frac{\sigma^2}{2} C(t, t') \end{aligned}$$

On the other hand, extremizing with respect to $\hat{M}, \hat{P}, \hat{C}, \hat{K}, \hat{L}$

$$\begin{aligned} M(t) &= \lim_{N \rightarrow \infty} N^{-1} \sum_i \langle x_i(t) \rangle_{\Omega} \\ P(t) &= \lim_{N \rightarrow \infty} N^{-1} \sum_i \langle i \hat{x}_i(t) \rangle_{\Omega} \\ C(t, t') &= \lim_{N \rightarrow \infty} N^{-1} \sum_i \langle x_i(t) x_i(t') \rangle_{\Omega} \\ K(t, t') &= \lim_{N \rightarrow \infty} N^{-1} \sum_i \langle x_i(t) \hat{x}_i(t') \rangle_{\Omega} \\ L(t, t') &= \lim_{N \rightarrow \infty} N^{-1} \sum_i \langle \hat{x}_i(t) \hat{x}_i(t') \rangle_{\Omega} \end{aligned}$$

Where the average $\langle (\cdot) \rangle_{\Omega}$ is to be taken against a measure defined by the exponent of the expression in Eq. (2.3) in the limit $h \rightarrow 0$.

From the latter equations, and taking the thermodynamical limit, one also notices that:

$$\begin{aligned} C(t, t') &= - \lim_{N \rightarrow \infty} N^{-1} \sum_i \frac{\delta^2 \overline{Z}[-]}{\delta \psi_i(t) \delta \psi_i(t')} \Big|_{\psi=0, h=0} \\ K(t, t') &= \lim_{N \rightarrow \infty} N^{-1} \sum_i \frac{\delta^2 \overline{Z}[-]}{\delta \psi_i(t) \delta h(t')} \Big|_{\psi=0, h=0} \\ L(t, t') &= - \lim_{N \rightarrow \infty} N^{-1} \sum_i \frac{\delta^2 \overline{Z}[-]}{\delta h(t) \delta h(t')} \Big|_{\psi=0, h=0} \\ P(t) &= - \lim_{N \rightarrow \infty} N^{-1} \sum_i \frac{\delta \overline{Z}[-]}{\delta h(t)} \Big|_{\psi=0, h=0} \end{aligned}$$

Given that $Z[\psi = 0, h] = 1$ for all h due to normalisation we conclude that $L(t, t') = 0$ for all t, t' , and $P(t) = 0$ for all t . We now set $\psi = 0$. We will also assume that initial conditions are chosen from identical distributions for all components x_i (i.e. $p_0^{(i)}(\cdot)$ does not depend on i). Then we have

$$\begin{aligned} \Omega &= \log \left[\int D[x, \hat{x}] p_0(x(0)) \exp \left\{ i \int dt \hat{x}(t) \left[\frac{\dot{x}(t)}{x(t)} - \left(1 - x(t) \right) + -h(t) - \mu M(t) \right] \right\} \right. \\ &\quad \left. \times \exp \left\{ -\sigma^2 \int dt dt' \left[\frac{1}{2} C(t, t') \hat{x}(t) \hat{x}(t') + i \gamma G(t, t') x(t) \hat{x}(t') \right] \right\} \right] \end{aligned} \quad (2.4)$$

where we have used the above saddle point results, and introduced $G(t, t') = iK(t, t')$.

2.2.2 The representative process

The final result for the generating functional post disorder average is therefore

$$Z_{eff} = \int D[x, \hat{x}] p_0(x(0)) \exp \left\{ i \int dt \hat{x}(t) \left[\frac{\dot{x}(t)}{x(t)} - (1 - x(t)) - h(t) - \mu M(t) \right] \right\} \\ \times \exp \left\{ -\sigma^2 \int dt dt' \left[\frac{1}{2} C(t, t') \hat{x}(t) \hat{x}(t') + i \gamma G(t, t') x(t) \hat{x}(t') \right] \right\}$$

This is recognised as the generating function of the effective dynamics

$$\dot{x}(t) = x(t) \left[1 - x(t) + \gamma \sigma^2 \int dt' G(t, t') x(t') + \mu M(t) + \eta(t) + h(t) \right]$$

where

$$G(t, t') = \left\langle \frac{\delta x(t)}{\delta h(t')} \right\rangle_*$$

$$\langle \eta(t) \eta(t') \rangle_* = \sigma^2 \langle x(t) x(t') \rangle_* \quad (2.5)$$

$$\langle x(t) \rangle_* = M(t)$$

and where $\langle \dots \rangle_*$ denotes an average over realizations of the effective dynamics. Given that this is to be evaluated at $h=0$ we can equivalently write

$$\dot{x}(t) = x(t) \left[1 - x(t) + \gamma \sigma^2 \int dt' G(t, t') x(t') + \mu M(t) + \eta(t) \right] \quad (2.6)$$

The equations in (2.5) determine $G(t, t')$, $C(t, t') = \langle x(t) x(t') \rangle_*$ and $M(t)$ self-consistently.

2.2.3 Fixed points analysis

We now assume that the system reaches a stationary state and that this stationary state does not depend on the initial condition (i.e., we assume absence of long-term memory). The response function G is then a function of time differences only, i.e. $G(t, t') = G(\tau)$, where $\tau = t - t'$. Causality dictates $G(\tau < 0) = 0$. Assuming further that the dynamics reaches a fixed point, $C(t, t')$ is constant (independent of t and t'); we write $C(t, t') \doteq q$.

Fixed points of the effective dynamics are given by the solutions of

$$x^* \left[1 - x^* + \gamma \sigma^2 q x^* + \mu M^* + \eta^* \right] = 0 \quad (2.7)$$

where we have written $\chi = \int_0^\infty d\tau G(\tau)$. We note that $\eta(t)$ becomes static Gaussian randomness η^* , at the fixed point, due to the self-consistency relation $\langle \eta(t)\eta(t') \rangle_* = \sigma^2 \langle x(t)x(t') \rangle_* \doteq \sigma^2 q$. We write $\eta^* = \sqrt{q}\sigma z$ with z a static Gaussian random variable of mean zero and unit variance.

Eq (2.7) always has the solution $x^* = 0$. The second solution

$$x^* = \frac{1 + \mu M + \sqrt{q}\sigma z}{1 - \gamma\sigma^2\chi}$$

is physical when this expression is non- negative. In the following we use

$$x(z) = \frac{1 + \mu M + \sqrt{q}\sigma z}{1 - \gamma\sigma^2\chi} \Theta\left(\frac{1 + \mu M + \sqrt{q}\sigma z}{1 - \gamma\sigma^2\chi}\right) \quad (2.8)$$

Where $\Theta(x)$ is the heavyside function, $\Theta(x) = 1$ for $x > 0$, and $\Theta(x) = 0$ elsewhere. The zero solution can be seen unstable when the expression in the Heavy-side function is positive, see below.

The order parameters χ, q, M are to be determined from the self- consistency relations depending on averages over the effective process.

$$\begin{aligned} \chi &= \frac{1}{\sqrt{q}\sigma} \left\langle \frac{\partial x(z)}{\partial z} \right\rangle_* \\ \langle x(z) \rangle_* &= M^* \\ q &= \langle (x(z))^2 \rangle_* \end{aligned}$$

That can be expressed as

$$\begin{aligned} \chi &= \frac{1}{\sqrt{q}\sigma} \int_{-\infty}^{\infty} Dz \frac{\partial x(z)}{\partial z} \\ M^* &= \int_{-\infty}^{\infty} Dz x(z) \\ q &= \int_{-\infty}^{\infty} Dz (x(z))^2 \end{aligned}$$

where $Dz = \frac{dz}{\sqrt{2\pi}} e^{-\frac{z^2}{2}}$

Only the non-zero fixed systems contribute to these integrals. We proceed under the assumption $1 - \gamma\sigma^2\chi > 0$. The range $x(z) > 0$ is then equivalent to $1 + \mu M + \sqrt{q}\sigma z > 0$ i.e $z > -\Delta$ where $\Delta = \frac{1 + \mu M^*}{\sqrt{q}\sigma}$.

This means that the fraction of surviving species is given by $\Phi = \int_{-\Delta}^{\infty} Dz$. In the integration range we have:

$$x(z) = \sqrt{q}\sigma \frac{\Delta + z}{1 - \gamma\sigma^2\chi}$$

Equations for χ, M^* and q then turn explicitly into closed non-linear integral equations:

$$\begin{aligned}
\chi &= \frac{1}{1 - \gamma\sigma^2\chi} \int_{-\infty}^{\Delta} Dz \\
M^* &= \sqrt{q}\sigma \frac{1}{1 - \gamma\sigma^2\chi} \int_{-\infty}^{\Delta} Dz (\Delta + z) \\
1 &= \frac{\sigma^2}{1 - \gamma\sigma^2\chi} \int_{-\infty}^{\Delta} Dz (\Delta + z)^2
\end{aligned} \tag{2.9}$$

Along the way, we have made the assumption $1 - \gamma\sigma^2\chi > 0$. This can be checked retrospectively from the numerical solution. It is also required self-consistently in the third relation in Eq. (2.9), as $M^* \geq 0$. We also note that the first relation in Eq. (2.9) then implies $\chi > 0$, which we will use below. We have $\Delta = \frac{1 + \mu M}{\sqrt{q}\sigma}$. We also have

$$\Phi = \int_{-\infty}^{\Delta} Dz \tag{2.10}$$

2.2.4 Numerical procedure

We define

$$w_l(\Delta) = \int_{-\infty}^{\Delta} Dz (\Delta - z)^l$$

And note

$$\begin{aligned}
w_0(\Delta) &= \frac{1}{2} \left[1 + \operatorname{erf}\left(\frac{\Delta}{\sqrt{2}}\right) \right] \\
w_1(\Delta) &= \frac{1}{2} \left[e^{-\frac{\Delta^2}{2}} \sqrt{\frac{2}{\pi}} + \Delta \left(1 + \operatorname{erf}\left(\frac{\Delta}{\sqrt{2}}\right) \right) \right] \\
w_2(\Delta) &= \frac{1}{2} (1 + \Delta^2) \left[1 + \operatorname{erf}\left(\frac{\Delta}{\sqrt{2}}\right) \right] + \frac{1}{\sqrt{2\pi}} e^{-\frac{\Delta^2}{2}} \Delta
\end{aligned}$$

This means

$$w_2(\Delta) = w_0(\Delta) + w_1(\Delta)$$

In order to find a solution we fix μ and γ , varying Δ and obtaining σ^2, q, χ, M as functions of Δ .

More precisely we find by dividing the square of the first equation in (2.9) by the third

$$\sigma^2 \chi^2 = \frac{w_0^2}{w_2} \tag{2.11}$$

From the first relation on the other hand,

$$\chi - \gamma\sigma^2\chi^2 = w_0$$

Putting this together we have

$$\chi = w_0 + \gamma \frac{w_0^2}{w_2}$$

Using this in Eq. (2.11) we find

$$\begin{aligned} \sigma^2 &= \frac{w_0^2}{w_2 \chi^2} \\ &= \frac{w_2}{(w_2 + \gamma w_0)^2} \end{aligned}$$

Next we introduce $b \doteq 1 - \gamma \sigma^2 \chi$ as an auxiliary variable, and note that

$$\begin{aligned} b &= 1 - \gamma \frac{w_2}{(w_2 + \gamma w_0)^2} \left(w_0 + \gamma \frac{w_0^2}{w_2} \right) \\ &= 1 - \gamma \frac{w_0}{w_2 + \gamma w_0} \\ &= \frac{w_2}{w_2 + \gamma w_0} \end{aligned}$$

From the second relation in Eq. (2.9) we have:

$$\sigma \sqrt{q} = \frac{bM}{w_1}$$

which, combined with $\Delta = \frac{1+\mu M}{\sqrt{q}\sigma}$ give

$$\begin{aligned} \frac{1}{M} &= \frac{\Delta}{w_1} b - \mu \\ &= \frac{\Delta}{w_1} \frac{w_0}{w_2 + \gamma w_0} - \mu \end{aligned}$$

Finally

$$q = \left(\frac{bM}{\sigma w_1} \right)^2$$

This gives M, q, Φ as a function of σ^2 in parametric form.

2.2.5 Order parameters

The notation x_i^* indicates abundances at stable fixed points.

The quantity $\phi = w_0$ is the fraction of surviving species, i.e., $\phi = \frac{1}{N} \sum_i \Theta(x_i^*)$, where $\Theta(x_i^*)$ is the Heaviside function, $\Theta(x_i^*) = 1$ for $x > 0$, and $\Theta(x_i^*) = 0$ for $x \leq 0$. To measure this in simulations one needs to apply a threshold, θ_{th} , and identify species i as surviving if $x_i \geq \theta_{th}$.

The quantity M is the mean abundance per species, $M = \frac{1}{N} \sum_i x_i^*$, i.e., the first moment of abundances. (The sum includes the species that have died out).

The quantity q is, $q = M = \frac{1}{N} \sum_i (x_i^*)^2$ (second moment of the distribution of abundances).

χ is a susceptibility and measures how strongly species abundances change if an external perturbation is applied. It is very hard to measure this directly in simulations.

The species abundance distribution (distribution of the x_i^* 's) has a delta peak at zero, plus a part which describes the surviving species

$$p(x) = (1 - \phi)\delta(x) + p_{\text{surv}}(x)$$

The weight of the delta-peak at $x = 0$ is $1 - \phi$, and we have $\int_0^\infty p_{\text{surv}}(x) = \phi$. The functional form of p_{surv} is a clipped Gaussian. More specifically, this is a Gaussian with the following properties:

- mean $\frac{1 + \mu M}{1 - \gamma \chi \sigma^2}$
- variance $\frac{q \sigma^2}{(1 - \gamma \sigma^2 \chi)^2}$

with cut off at $x = 0$.

2.2.6 Linear stability of steady states

The linear stability analysis of (2.8) reveals:

- Perturbations around zero fixed points decay. The zero fixed point is not stable if the object $1 + \mu M^* + \sqrt{q} \sigma z$ is positive, justifying retrospectively that we use in that case the non-zero solution for x^* .
- Perturbations around the non-zero fixed point diverge when $\phi \sigma^2 = (1 - \gamma \chi \sigma^2)^2$. One finds $\phi \sigma^2 < (1 - \gamma \chi \sigma^2)^2$ in the stable phase.

For the non-zero solution, the condition $\phi \sigma^2 = (1 - \gamma \chi \sigma^2)^2$ leads to $\Delta = 0$. To see this we insert this condition into $1 = \frac{\sigma^2}{1 - \gamma \sigma^2 \chi} \int_{-\infty}^{\Delta} Dz (\Delta - z)^2$ and find

$$\phi = \int_{-\infty}^{\Delta} Dz (\Delta - z)^2$$

On the other hand we also have $\phi = \int_{-\infty}^{\Delta} Dz$. Comparing the two expressions gives $\Delta = 0$ and hence $\phi = \frac{1}{2}$.

Using this, we have

$$\begin{aligned} 2\chi &= \frac{1}{1 - \gamma \sigma^2 \chi} \\ 2 &= \frac{\sigma^2}{(1 - \gamma \sigma^2 \chi)^2} \end{aligned} \tag{2.12}$$

from which we find $\chi^2 = \frac{1}{2\sigma^2}$. Using $\chi > 0$ we have $\chi = \frac{1}{\sqrt{2}\sigma}$. Substituting this in the first relation in Eq. (2.12) in turn leads to

$$\sigma_c^2(\gamma) = \frac{2}{(1+\gamma)^2} \quad (2.13)$$

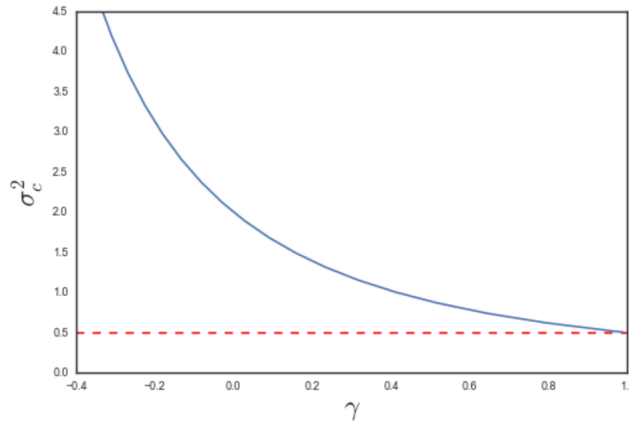


Figure 1: Critical value of the variance of interactions as a function of correlation parameter γ . The red dashed line shows the smallest possible value of σ_c^2 , obtained at $\gamma = 1$.

The linear stability results are shown to be independent from the mean of interactions as long as $\mu < 0$. While the outcome of the dynamics beyond the stable regime actually depends on the mean of interactions. From the Dynamical mean field theory analysis it is also possible to determine a phase diagram (σ, μ) of the GLV model, given a fixed value of γ (7). In the limit of large system size, three dynamical phases are found.

- Phase 1: Unique Fixed Point phase. Any given system admits a unique, stable fixed point. This equilibrium state is stable to local and global perturbations, up to a critical value of variance that can be computed according to (2.13).
- Phase 2: Multiple attractors. Above the critical threshold $\sigma_c^2(\gamma)$ the system is not linearly stable anymore. The outcome will be history dependent. For a given system, it can be a fixed point or in general a dynamical attractor, but it will depend on initial conditions and the specific dynamics.
- Phase 3: Unbounded Growth: When the average interaction is positive $\mu > 0$, or for sufficiently large variance σ^2 , cooperation prevail on single species saturation, and the system is driven to a state where the biomass explodes. If we fix a lower mean and increase the variance, at some point a portion of the community of species will have cooperative interactions stronger than their own saturation and this subgroup of species will thus grow without bound, even though all the other species will die out. The borders between phases can be computed analytically: I/II and I/III are exact, but II/III is only approximate (7).

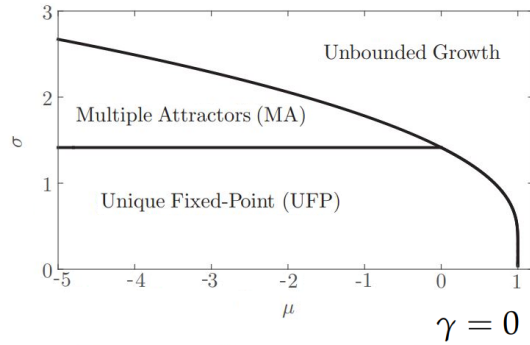


Figure 2: Qualitative phase diagram (σ, μ) for $\gamma = 0$. With $\sigma = \sqrt{N} \text{std}(z_{ij})$ and μ the mean of interactions.

2.2.7 Results of the model

Through the generating functional approach, the study of a large size community reduces to the stochastic dynamics of an effective species, while still being representative for the whole statistical ensemble determined by equations (1.3) and (1.4). A phase diagram can be computed, showing the complexity of the possible scenarios, from unique or multiple fixed points to chaotic regimes, depending on the structural parameters and nature of interactions. The non-zero steady solution results to be stable withing a specific range of variability for the interactions, from zero up to a critical value $\sigma_c^2(\gamma)$ that increases as γ increases, as shown in Figure 1. This critical value separates stable fixed-point regimes from phases in which characteristic quantities such as the biomass and individual species concentrations can diverge or fluctuate in time, as it will be discussed in comparison with numerical solutions. For $\gamma = 1$ (0 % of predator-prey pairs) we find the smallest range of stability for the variance $\sigma^2 < \sigma_c^2 = 0.5$, for $\gamma = 0$ (50 % of predator-prey pairs) we find $\sigma_c^2 = 2$, while for $\gamma = -1$ (100 % of predator-prey pairs) the steady state is stable for any possible finite value of variance. This result shows how predator prey interactions actually promote the stability of the community, coherently with the results found from random matrix theory. One can also investigate the effect that the model parameters σ , μ and γ have on the properties of the steady state such as the fraction of surviving species ϕ and the average density of species M , also referred as biomass.

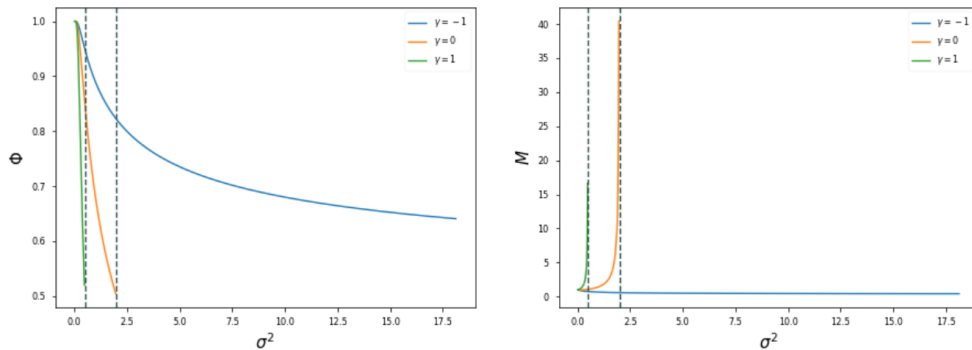


Figure 3: Figures on the left and right show respectively the fraction of surviving species ϕ and total biomass M as a function of the variance σ^2 , for different values of γ . Vertical dashed gray lines indicate $\sigma_c^2(0)$ and $\sigma_c^2(1)$.

Results in Figure 3 can be interpreted in terms of complexity (measured by σ^2 and diversity (measured by γ) of the ecosystem, within the theoretical model. The fraction of surviving species ϕ is a decreasing function of the variance, independently of the percentage of predator-prey pairs in the food web. On the other hand, the biomass is enhanced by diversity (for γ equal to 0 and 1), while it stabilizes to a finite value when all interaction pairs are of predator-prey type. Therefore while the network is destabilized by an increasing variance, the community reduces to a smaller size. The total biomass increases as the diversity of species interaction is increased. The size of the remaining ecosystem and stability are thus positively correlated. Communities with a large number of surviving species are hence more likely to be stable than smaller ones. We can notice that the community is stable when at least 50% of species survive, and unstable otherwise, as shown in the analytical solution. Numerical studies of the GLV have shown to be coherent with these theoretical predictions (3).

2.2.8 Cavity Method

Consider the GLV model in its general form, looking at dynamics of the population density $x_i(t) \geq 0$ for a system of N species $i = 1, \dots, N$.

$$\frac{dx_i}{dt} = x_i \left[1 - x_i + \sum_{j \neq i} z_{ij} x_j + h_i(t) \right] \quad (2.14)$$

Where the parameters involved are equivalent to the ones discussed for equation (1.2). An external field $h_i(t)$ is added to define the response of the system to a perturbation. The elements $\{z_{ij}\}_{i \neq j}$ follow in pairs a bivariate Gaussian distribution

$$z_{ij} = \frac{\mu}{N} + \sigma w_{ij} \quad z_{ji} = \frac{\mu}{N} + \sigma w_{ji} \quad (2.15)$$

Where (w_{ij}, w_{ji}) follow a bivariate gaussian with mean $\underline{0}$ and covariance matrix

$$\Sigma = \frac{1}{N} \begin{pmatrix} 1 & \gamma \\ \gamma & 1 \end{pmatrix} \quad (2.16)$$

The result does not depend on the particular distribution for the z_{ij} 's but only on the existence of the first two cumulants. The initial conditions are sampled from a joint distribution $P\{x_i(t=0)\} = \prod_{i=1, \dots, N} (x_i(t=0))$. The notation $\langle \langle \dots \rangle \rangle$ refers to the average over the couplings $\{z_{ij}\}_{i \neq j}$ and initial conditions $\{x_i(0)\}_{i=1, \dots, N}$.

For given parameters μ, σ, γ and system size N , consider a system whose interaction couplings and initial conditions are drawn for every species. We can define the deterministic trajectories $\{x_i(t)\}_{i=1, \dots, N}$. We now add a new species with density x_0 along with newly sampled interactions $\{z_{i0}, z_{0i}\}_{i=1, \dots, N}$ with the existing system, and comparing the properties of the solution with N species to that with $N+1$ species, requiring that the new species has the same properties as the rest. If N is large enough, the impact of this new species on the previous trajectories is a small perturbation and therefore we only consider linear response for the trajectories $\{\tilde{x}_i(t)\}_{i=1, \dots, N}$ in the presence of new species '0':

$$\tilde{x}_i(t) = x_i(t) + \sum_{j=1,\dots,N} \int_0^t \frac{\delta x_i(t)}{\delta h_j(s)} \Big|_{h=0} z_{j0} x_0(s) ds \quad (2.17)$$

The partial derivative are to be understood in a functional sense. We introduce the notation for the response function:

$$\chi_{ij}(t, s) = \frac{\delta x_i(t)}{\delta h_j(s)} \Big|_{h=0} \quad (2.18)$$

We can now plug these new trajectories in the equation for x_0 :

$$\dot{x}_0 = x_0(1 - x_0 + \sum_{i \neq 0} z_{0i} \tilde{x}_i + h_0(t)) \quad (2.19)$$

The interaction term can be rewritten exploiting the definition of the z_{ij} 's. The summations \sum_j stand for $\sum_{j=1,\dots,N}$.

$$\begin{aligned} \sum_j z_{0j} \tilde{x}_j &= \frac{\mu}{N} \sum_i x_i(t) + \frac{\mu}{N} \sum_{ij} \int_0^t \chi_{ij}(t, s) \left(\frac{\mu}{N} + \sigma w_{j0} \right) x_0(s) ds \\ &+ \sigma \sum_i w_{0i} x_i(t) + \sigma \sum_{ij} w_{0i} \int_0^t \chi_{ij}(t, s) \left(\frac{\mu}{N} + \sigma w_{j0} \right) x_0(s) ds \end{aligned}$$

We take the large N limit and analyze the statistical properties of all terms, by performing an average over coupling parameters and initial conditions. Since by construction the trajectories $\{x_i(t)\}_{i=1,\dots,N}$ are independent from z_{i0} and z_{0i} , one can use central limit arguments. We look at the response function terms $\sum_{ij} w_{0i} \chi_{ij}(t, s) w_{j0}$. The different $\chi_{ij}(t, s)$ are random functions that will depend on the initial conditions $x_{i \neq 0}(0)$ and the interaction matrix $\{z_{ij}\}_{i,j > 0}$, but are otherwise independent from z_{i0} and z_{0i} . We first treat the diagonal part. According to the central limit theorem and up to second order contribution, the term $\sum_i w_{0i} \chi_{ii}(t, s) w_{i0}$ will converge towards its average:

$$S\langle \chi_{ii} w_{i0} w_{0i} \rangle = S\langle \chi_{ii} \rangle \langle w_{i0} w_{0i} \rangle = \gamma \langle \chi_{ii} \rangle \quad (2.20)$$

while the non diagonal part $\sum_{i \neq j} w_{0i} \chi_{ij}(t, s) w_{j0}$ has zero average since the coupled parameters are only correlated in pairs, i.e $\langle w_{0i} w_{j0} \rangle_{i \neq j} = 0$. To determine the scaling of its fluctuations we look at the variance of each term in the sum $\langle \chi_{ij} \rangle_{i \neq j}^2 \langle w_{j0}^2 w_{0i}^2 \rangle_{i \neq j}$, it can be shown by perturbation theory in the strength of interactions that χ_{ij} is of order $N^{-1/2}$ for $i \neq j$. Regrouping the scalings we obtain that the off-diagonal term $\sum_{i \neq j} w_{0i} \chi_{ij}(t, s) w_{j0}$ behaves as

$$N(N-1) \langle \chi_{ij} \rangle_{i \neq j} \langle w_{i0} w_{0i} \rangle_{i \neq j} + \sqrt{N(N-1)} \sqrt{\langle \chi_{ij} \rangle_{i \neq j}^2} \sqrt{\langle w_{j0}^2 w_{0i}^2 \rangle_{i \neq j}} Z \sim 0 + \frac{1}{\sqrt{N}} Z$$

where Z is a standard Gaussian, thus the off-diagonal term induces correction of $O(N^{-\frac{1}{2}})$ that are negligible in the thermodynamical limit. Using the same procedure for the remaining terms, we get

$$\dot{x}_0 = x_0 \{1 - x_0 + \mu \langle x_i(t) \rangle + \sigma \eta(t) + \gamma \sigma^2 \int_0^t \chi(t,s) x(s) ds + h(t)\} \quad (2.21)$$

Where η is a Gaussian noise with zero mean and covariance $\langle \eta(t) \eta(s) \rangle_\eta = \langle x_i(t) x_i(s) \rangle$. But once species "0" has been added to the system it is in no way different from the other species, so we may drop the subscript 0 to obtain the dynamical mean field theory:

$$\dot{x} = x \{1 - x + \mu m(t) + \sigma \eta(t) + \gamma \sigma^2 \int_0^t \chi(t,s) x(s) ds + h(t)\} \quad (2.22)$$

With the following self consistent equations for the average population $m(t)$, noise correlator $C(t,s) = \langle \eta(t) \eta(s) \rangle_\eta$, and response function $\chi(t,s)$.

$$\begin{cases} m(t) &= \mathbb{E}[x(t)] \\ C(t,s) &= \mathbb{E}[x(t)x(s)] \\ \chi(t,s) &= \mathbb{E}\left[\frac{\delta x(t)}{\delta h(s)}\right]_{h=0} \end{cases}$$

In these definitions, the averages $\mathbb{E}[(\cdot)]$ are now taken with respects to the noise trajectories η and the initial condition $x(0)$. Finally, from an deterministic system of coupled differential equations in N degrees of freedom we ended up with a one-body stochastic self-consistent differential equation. It has been mathematically proven for spin glasses that in the thermodynamical limit $N \rightarrow \infty$, there is a convergence in law between the statistics of the two descriptions (5).

2.3 Linear quadratic systems

Removing the assumption of boundness for the action profile space $A_i = [0, \infty[$, the equations of the learning process can be rewritten as

$$a_i^t = \max \{0, \alpha_i + b_i^t\} \quad (2.23)$$

$$b_i^{t+1} = \begin{cases} b_i^t & \text{if } a_i^t = 0 \\ \sum_{j \in I} z_{ij} a_j^t & \text{if } a_i^t > 0 \end{cases} \quad (2.24)$$

with initial conditions b_i^0 .

The process is deterministic, the only stochasticity being in the initial conditions and in the quenched disorder determining the structure of the network and the parameters α_i s. Using the learning process,

$$\begin{aligned} a_i^{t+1} &= \max \left\{ 0, \alpha_i + b_i^{t+1} \right\} \\ &= \max \left\{ 0, \alpha_i + b_i^t + \Theta(\alpha_i + b_i^t) \left[\sum_{j \in I} z_{ij} a_j^t - b_i^t \right] \right\} \\ &= \max \left\{ 0, \Theta(a_i^t) \left[\alpha_i + \sum_{j \in I} z_{ij} a_j^t \right] \right\} \end{aligned} \quad (2.25)$$

and adding a time-dependent external field h_i^t , we obtain a single equation for actions,

$$a_i^{t+1} = \max \left\{ 0, \Theta(x_i^t) \left[\alpha_i + \sum_{j \in I} z_{ij} a_j^t + h_i^t \right] \right\}. \quad (2.26)$$

2.3.1 Generating Functional approach

We introduce a dynamical partition function $Z[\boldsymbol{\psi}]$ using a path integral approach as follows

$$\begin{aligned}
Z[\boldsymbol{\psi}] &= \left\langle \left\langle \exp \left(i \sum_i \sum_t \psi_i^t a_i^t \right) \right\rangle_{\text{i.c.}} \right\rangle_z \\
&= \left\langle \int D\mathbf{a} \int D\boldsymbol{\alpha} \prod_i f(\alpha_i) \prod_i p(a_i^0) \exp \left(i \sum_i \sum_t \psi_i^t a_i^t \right) \right. \\
&\quad \left. \times \prod_{i,t} \delta \left(a_i^{t+1} - \max \left\{ 0, \Theta(a_i^t) \left[\alpha_i + \sum_{j \in I} z_{ij} a_j^t + h_i^t \right] \right\} \right) \right\rangle_z \\
&= \left\langle \int D\mathbf{a} \int D\hat{\mathbf{a}} \int D\boldsymbol{\alpha} \prod_i f(\alpha_i) \prod_i p(a_i^0) \exp \left(i \sum_i \sum_t \psi_i^t a_i^t \right) \right. \\
&\quad \left. \times e^{\sum_i \sum_t \hat{a}_i^t (a_i^{t+1} - \max \{ 0, \Theta(a_i^t) [\alpha_i + \sum_{j \in I} z_{ij} a_j^t + h_i^t] \})} \right\rangle_z \\
&= \left\langle \int D\mathbf{a} \int D\hat{\mathbf{a}} \int D\mathbf{y} \int D\boldsymbol{\alpha} \prod_i f(\alpha_i) \prod_i p(a_i^0) \exp \left(i \sum_i \sum_t \psi_i^t a_i^t \right) \right. \\
&\quad \left. \times e^{i \sum_i \sum_t \hat{a}_i^t (a_i^{t+1} - \max \{ 0, \Theta(a_i^t) y_i^t \})} \right. \\
&\quad \left. \times \prod_{i,t} \delta \left(y_i^t - \alpha_i - \sum_{j \in I} z_{ij} a_j^t - h_i^t \right) \right\rangle_z \\
&= \left\langle \int D\mathbf{a} D\hat{\mathbf{a}} D\mathbf{y} D\hat{\mathbf{y}} \int D\boldsymbol{\alpha} \prod_i f(\alpha_i) \prod_i p(a_i^0) \right. \\
&\quad \left. \times e^{i \sum_i \sum_t \psi_i^t a_i^t + i \sum_i \sum_t \hat{a}_i^t (a_i^{t+1} - \max \{ 0, \Theta(a_i^t) y_i^t \}) + i \sum_i \sum_t \hat{y}_i^t (y_i^t - \alpha_i - \sum_{j \in I} z_{ij} a_j^t - h_i^t)} \right\rangle_z.
\end{aligned}$$

Reordering terms and introducing $g(a, y) = \max(0, \Theta(a) y)$,

$$\begin{aligned}
Z[\boldsymbol{\psi}] &= \left\langle \int D\mathbf{a} \int D\hat{\mathbf{a}} \int D\mathbf{y} \int D\hat{\mathbf{y}} \int D\boldsymbol{\alpha} \prod_i f(\alpha_i) \prod_i p(a_i^0) \right. \\
&\quad \left. \times e^{i \sum_i \sum_t \psi_i^t a_i^t + i \sum_i \sum_t \{ \hat{a}_i^t (a_i^{t+1} - g(a_i^t, y_i^t)) + \hat{y}_i^t (y_i^t - \alpha_i - h_i^t) \}} \prod_{i < j} e^{-i \sum_t (\hat{y}_i^t z_{ij} a_j^t + \hat{y}_j^t z_{ji} a_i^t)} \right\rangle_z \\
&= \int D\mathbf{a} \int D\hat{\mathbf{a}} \int D\mathbf{y} \int D\hat{\mathbf{y}} \int D\boldsymbol{\alpha} \prod_i f(\alpha_i) \prod_i p(a_i^0) \\
&\quad \times e^{i \sum_i \sum_t \psi_i^t a_i^t + i \sum_i \sum_t \{ \hat{a}_i^t (a_i^{t+1} - g(a_i^t, y_i^t)) + \hat{y}_i^t (y_i^t - \alpha_i - h_i^t) \}} \\
&\quad \times \left\langle \prod_{i < j} e^{-i \sum_t (\hat{y}_i^t z_{ij} a_j^t + \hat{y}_j^t z_{ji} a_i^t)} \right\rangle_z
\end{aligned}$$

In order to perform the average over the disorder we notice that $z_{ij} = \frac{\mu}{N} + \frac{\sigma}{\sqrt{N}} w_{ij}$ with w_{ij} normal random variables. More precisely we assume that random variables on different links are independent but those on the same link are correlated. Let us assume that $\mathcal{N}(w_{ij}, w_{ji})$ is a bivariate normal distribution with zero mean

and covariance $\Sigma = \begin{pmatrix} 1 & \gamma \\ \gamma & 1 \end{pmatrix}$, that is $\langle w_{ij}^2 \rangle = \langle w_{ji}^2 \rangle = 1$ and $\langle w_{ij} w_{ji} \rangle = \gamma$. Performing the gaussian average, the interaction term becomes

$$\begin{aligned} \left\langle \prod_{i<j} e^{-i \Sigma_t (\hat{y}_i^t z_{ij} a_j^t + \hat{y}_j^t z_{ji} a_i^t)} \right\rangle_z &= \prod_{i<j} \int d\mathcal{N}(w_{ij}, w_{ji}) e^{-i \frac{\sigma}{\sqrt{N}} \Sigma_t (\hat{y}_i^t w_{ij} a_j^t + \hat{y}_j^t w_{ji} a_i^t)} \\ &= \prod_{i<j} e^{-\frac{\sigma^2}{2N} \Sigma_{tt'} (\hat{y}_i^t a_j^t \hat{y}_i^{t'} a_j^{t'} + \hat{y}_j^t a_i^t \hat{y}_j^{t'} a_i^{t'} + 2\gamma \hat{y}_i^t a_j^t \hat{y}_j^{t'} a_i^{t'})}. \end{aligned}$$

Now we obtained a process on N degrees of freedom in which there is no disorder anymore

$$\begin{aligned} Z[\boldsymbol{\psi}] &= \int D\mathbf{a} \int D\hat{\mathbf{a}} \int D\mathbf{y} \int D\hat{\mathbf{y}} \int D\alpha \prod_i f(\alpha_i) \prod_i p(a_i^0) \\ &\quad \times e^{i \Sigma_i \Psi_i^t a_i^t + i \Sigma_i \Sigma_t \{ \hat{a}_i^t (a_i^{t+1} - g(a_i^t, y_i^t)) + \hat{y}_i^t (y_i^t - \alpha_i - h_i^t) \}} \\ &\quad \times \prod_{i<j} e^{-i \frac{\mu}{N} \Sigma_t (\hat{y}_i^t a_j^t + \hat{y}_j^t a_i^t) - \frac{\sigma^2}{2N} \Sigma_{tt'} (\hat{y}_i^t a_j^t \hat{y}_i^{t'} a_j^{t'} + \hat{y}_j^t a_i^t \hat{y}_j^{t'} a_i^{t'} + 2\gamma \hat{y}_i^t a_j^t \hat{y}_j^{t'} a_i^{t'})}. \end{aligned}$$

It is now convenient to introduce collective averages and correlation functions by enforcing the following definitions

$$\begin{aligned} M(t) &= \frac{1}{N} \sum_i a_i(t) \\ Y(t) &= \frac{i}{N} \sum_i \hat{y}_i(t) \\ Q_{11}(t, t') &= \frac{1}{N} \sum_i a_i(t) a_i(t') \\ Q_{21}(t, t') &= \frac{1}{N} \sum_i \hat{y}_i(t) a_i(t') \\ Q_{12}(t, t') &= \frac{1}{N} \sum_i a_i(t) \hat{y}_i(t') \\ Q_{22}(t, t') &= \frac{1}{N} \sum_i \hat{y}_i(t) \hat{y}_i(t') \end{aligned}$$

by means of functional delta functions of the type

$$\delta \left(N Q_{11}(t, t') - \sum_i a_i(t) a_i(t') \right) = \int D\tilde{Q}_{11} e^{iN \Sigma_{tt'} (\tilde{Q}Q - \tilde{Q}N^{-1} \Sigma_i a_i(t) a_i(t'))}$$

and we get

$$\begin{aligned}
& e^{-i\frac{\mu}{N}\sum_t(\hat{y}_i^t a_i^t + \hat{y}_i^t a_i^t) - \frac{\sigma^2}{2N}\sum_{tt'}\sum_{ij}(\hat{y}_i^t a_i^t \hat{y}_i^{t'} a_i^{t'} + \gamma \hat{y}_i^t a_i^t \hat{y}_i^{t'} a_i^{t'})} = \\
& \int D\tilde{Q}_{11} \int D\tilde{Q}_{12} \int D\tilde{Q}_{21} \int D\tilde{Q}_{22} \int DQ_{11} \int DQ_{12} \int DQ_{21} \int DQ_{22} \int D\tilde{M} \\
& \times \int D\tilde{Y} \int DM \int DY e^{iN\sum_t(\tilde{M}M - \tilde{M}N^{-1}\sum_i a_i^t)} e^{iN\sum_t(\tilde{Y}Y - i\tilde{Y}N^{-1}\sum_i \hat{y}_i^t)} \\
& \times e^{iN\sum_{tt'}(\tilde{Q}_{11}Q_{11} - \tilde{Q}_{11}N^{-1}\sum_i a_i^t a_i^{t'})} e^{iN\sum_{tt'}(\tilde{Q}_{12}Q_{12} - \tilde{Q}_{12}N^{-1}\sum_i a_i^t \hat{y}_i^{t'})} \\
& \times e^{iN\sum_{tt'}(\tilde{Q}_{22}Q_{22} - \tilde{Q}_{21}N^{-1}\sum_i \hat{y}_i^t \hat{y}_i^{t'})} e^{iN\sum_{tt'}(\tilde{Q}_{21}Q_{21} - \tilde{Q}_{21}N^{-1}\sum_i \hat{y}_i^t a_i^{t'})} \\
& \times e^{-\frac{\sigma^2 N}{2}\sum_{tt'}(Q_{22}(t,t')Q_{11}(t,t') + \gamma Q_{21}(t,t')Q_{12}(t,t')) - \mu N\sum_t M(t)Y(t)}.
\end{aligned}$$

The full dynamical partition function becomes

$$\begin{aligned}
Z[\boldsymbol{\psi}] &= \int D\tilde{M} \int D\tilde{Y} \int DM \int DY \int D\tilde{Q}_{11} \int D\tilde{Q}_{12} \int D\tilde{Q}_{21} \int D\tilde{Q}_{22} \int DQ_{11} \int DQ_{12} \int DQ_{21} \\
& \times \int DQ_{22} \int D\mathbf{a} D\hat{\mathbf{a}} D\mathbf{y} D\hat{\mathbf{y}} D\boldsymbol{\alpha} e^{\sum_i \{ \log f(\alpha_i) + \log p(a_i^0) + i\sum_t \psi_i^t a_i^t + i\sum_t \{ \hat{a}_i^t (a_i^{t+1} - g(a_i^t, y_i^t)) + \hat{y}_i^t (y_i^t - \alpha_i - h_i^t) \} \}} \\
& \times e^{-i\sum_t \sum_i (\tilde{M}(t)a_i^t + \tilde{Y}(t)i\hat{y}_i^t) + N\sum_t (\tilde{M}(t)iM(t) + \tilde{Y}(t)iY(t) - \mu M(t)Y(t))} \\
& \times e^{-i\sum_t \sum_{tt'} (\tilde{Q}_{11}(t,t')a_i^t a_i^{t'} + \tilde{Q}_{12}(t,t')a_i^t \hat{y}_i^{t'} + \tilde{Q}_{21}(t,t')\hat{y}_i^t a_i^{t'} + \tilde{Q}_{22}(t,t')\hat{y}_i^t \hat{y}_i^{t'})} \\
& \times e^{N\sum_{tt'} (i\tilde{Q}_{11}Q_{11} + i\tilde{Q}_{12}Q_{12} + i\tilde{Q}_{21}Q_{21} + i\tilde{Q}_{22}Q_{22} - \frac{\sigma^2}{2}Q_{22}(t,t')Q_{11}(t,t') - \frac{\sigma^2}{2}\gamma Q_{21}(t,t')Q_{12}(t,t'))}
\end{aligned}$$

which can be written as

$$\begin{aligned}
Z[\boldsymbol{\psi}] &= \int D\tilde{M} \int DM \int D\tilde{Y} \int DY \int D\tilde{Q}_{11} \int D\tilde{Q}_{12} \int D\tilde{Q}_{21} \int D\tilde{Q}_{22} \int DQ_{11} \\
& \times \int DQ_{12} \int DQ_{21} \int DQ_{22} e^{N(\boldsymbol{\Psi} + \boldsymbol{\Phi} + \boldsymbol{\Omega} + O(N^{-1}))}
\end{aligned} \tag{2.27}$$

with

$$\begin{aligned}
\boldsymbol{\Omega} &= \frac{1}{N} \sum_i \log \left[\int Da_i D\hat{a}_i Dy_i D\hat{y}_i D\alpha_i f(\alpha_i) p(a_i^0) e^{i\sum_t \psi_i^t a_i^t + i\sum_t \{ \hat{a}_i^t (a_i^{t+1} - g(a_i^t, y_i^t)) + \hat{y}_i^t (y_i^t - \alpha_i - h_i^t) \}} \right. \\
& \left. \times e^{-i\sum_t (\tilde{M}(t)a_i^t + \tilde{Y}(t)i\hat{y}_i^t) - i\sum_{tt'} (\tilde{Q}_{11}(t,t')a_i^t a_i^{t'} + \tilde{Q}_{12}(t,t')a_i^t \hat{y}_i^{t'} + \tilde{Q}_{21}(t,t')\hat{y}_i^t a_i^{t'} + \tilde{Q}_{22}(t,t')\hat{y}_i^t \hat{y}_i^{t'})} \right],
\end{aligned}$$

$$\begin{aligned}
\boldsymbol{\Phi} &= i \sum_t (\tilde{M}(t)X(t) + \tilde{Y}(t)Y(t)) + i \sum_{tt'} (\tilde{Q}_{11}(t,t')Q_{11}(t,t') \\
& + \tilde{Q}_{12}(t,t')Q_{12}(t,t') + \tilde{Q}_{21}(t,t')Q_{21}(t,t') + \tilde{Q}_{22}(t,t')Q_{22}(t,t'))
\end{aligned}$$

and

$$\boldsymbol{\Psi} = -\mu \sum_t M(t)Y(t) - \frac{\sigma^2}{2} \sum_{tt'} (Q_{22}(t,t')Q_{11}(t,t') + \gamma Q_{21}(t,t')Q_{12}(t,t')).$$

At the saddle point, when $N \rightarrow \infty$, the individual-dependent part assumes a limiting form

$$\Omega = \log \left[\int DaD\hat{a}DyD\hat{y}D\alpha f(\alpha) p(a^0) e^{i\sum_i \psi^t a^t + i\sum_i \{\hat{a}^t (a^{t+1} - g(a^t, y^t)) + \hat{y}^t (y^t - \alpha - h^t)\}} \right. \\ \left. \times e^{-i\sum_i (\tilde{M}(t)a^t + \tilde{Y}(t)i\hat{y}^t) - i\sum_{t,t'} (\tilde{Q}_{11}(t,t')a^t a^{t'} + \tilde{Q}_{12}(t,t')a^t \hat{y}^{t'} + \tilde{Q}_{21}(t,t')\hat{y}^t a^{t'} + \tilde{Q}_{22}(t,t')\hat{y}^t \hat{y}^{t'})} \right]. \quad (2.28)$$

Moreover, performing the extremization with respect to M , Y , Q_{11} , Q_{12} , Q_{21} and Q_{22} , we get the conditions

$$\begin{aligned} i\tilde{M}(t) &= \mu Y(t) \\ i\tilde{Y}(t) &= \mu M(t) \\ i\tilde{Q}_{11}(t, t') &= \frac{\sigma^2}{2} Q_{22}(t, t') \\ i\tilde{Q}_{12}(t, t') &= \frac{\sigma^2}{2} \gamma Q_{21}(t, t') \\ i\tilde{Q}_{21}(t, t') &= \frac{\sigma^2}{2} \gamma Q_{12}(t, t') \\ i\tilde{Q}_{22}(t, t') &= \frac{\sigma^2}{2} Q_{11}(t, t') \end{aligned}$$

On the other hand, extremizing with respect to \tilde{Q}_{11} , we obtain

$$\begin{aligned} iQ_{11}(t, t') &= \frac{\delta \Omega}{\delta Q_{11}} \\ &= i \frac{1}{Z_{11}} \int DaD\hat{a}DyD\hat{y} p(a^0) (a^t a^{t'}) \\ &\quad \times e^{i\sum_i \{\psi^t a^t + \hat{a}^t (a^{t+1} - g(a^t, y^t)) + \hat{y}^t (y^t - \alpha - h^t) - \tilde{M}(t)a^t - \tilde{Y}(t)i\hat{y}^t\}} \\ &\quad \times e^{-i\sum_i \{\sum_{t'} (\tilde{Q}_{11}(t,t')a^t a^{t'} + \tilde{Q}_{12}(t,t')a^t \hat{y}^{t'} + \tilde{Q}_{21}(t,t')\hat{y}^t a^{t'} + \tilde{Q}_{22}(t,t')\hat{y}^t \hat{y}^{t'})\}} \\ &= i \langle a^t a^{t'} \rangle_{\Omega} \end{aligned}$$

which is the expected behavior of product $a^t a^{t'}$ performed over a sample dynamical process in the $N \rightarrow \infty$ limit. This is the usual definition of correlation function.

Performing the other extremizations we obtain

$$\begin{aligned}
M(t) &= \langle a^t \rangle_{\Omega} \\
Y(t) &= \langle i\hat{y}^t \rangle_{\Omega} = - \left. \frac{\delta}{\delta h^t} 1 \right|_{\psi=0} = 0 \\
Q_{11}(t, t') &= \langle a^t a^{t'} \rangle_{\Omega} \\
Q_{12}(t, t') &= \langle a^t \hat{y}^{t'} \rangle_{\Omega} = \frac{\delta \langle a^t \rangle_{\Omega}}{\delta h^{t'}} \\
Q_{21}(t, t') &= \langle \hat{y}^t a^{t'} \rangle_{\Omega} = \frac{\delta \langle a^{t'} \rangle_{\Omega}}{\delta h^t} \\
Q_{22}(t, t') &= \langle \hat{y}^t \hat{y}^{t'} \rangle_{\Omega} = \left. \frac{\delta^2}{\delta h^t \delta h^{t'}} 1 \right|_{\psi=0} = 0.
\end{aligned}$$

2.3.2 The representative process

Using this set of results, we can interpret Ω as the dynamical partition function of a representative single-degree of freedom

$$\begin{aligned}
Z_{\text{eff}}[\psi = 0] &= \int DaD\hat{a}DyD\hat{y}D\alpha f(\alpha) p(a^0) e^{\sum_t \{i\hat{a}^t (a^{t+1} - g(a^t, y^t)) + \hat{y}^t (y^t - \alpha - h^t - \mu M(t))\}} \\
&\quad \times e^{\sum_t \left\{ -\frac{\sigma^2}{2} \sum_{t'} (\gamma a^t Q_{21}(t, t') \hat{y}^{t'} + \gamma \hat{y}^t Q_{12}(t, t') a^{t'} + \hat{y}^t Q_{11}(t, t') \hat{y}^{t'}) \right\}} \\
&= \int DaDyD\hat{y}D\alpha f(\alpha) p(a^0) \prod_t \delta(a^{t+1} - g(a^t, y^t)) \\
&\quad \times e^{\sum_t \left\{ \hat{y}^t (y^t - \alpha - h^t - \mu M(t)) - \frac{\sigma^2}{2} \sum_{t'} (2\gamma \hat{y}^t Q_{12}(t, t') a^{t'} + \hat{y}^t Q_{11}(t, t') \hat{y}^{t'}) \right\}} \\
&= \int DaDyD\hat{y}D\alpha f(\alpha) p(a^0) \prod_t \delta(a^{t+1} - g(a^t, y^t)) \\
&\quad \times e^{\sum_t \left\{ \hat{y}^t (y^t - \alpha - h^t - \mu M(t) - \frac{\sigma^2}{2} \sum_{t'} [2\gamma Q_{12}(t, t') a^{t'} + Q_{11}(t, t') \hat{y}^{t'}]) \right\}}.
\end{aligned}$$

The representative process, which is parametrized by the variable α , involves the local field y^t ,

$$a^{t+1} = g\left(a^t, \alpha + h^t + \mu M(t) + \sigma^2 \gamma \sum_{t'} Q_{12}(t, t') a^{t'} + \eta^t\right) \quad (2.29)$$

with $\langle \eta^t \rangle = 0$ and $\langle \eta^t \eta^{t'} \rangle = \sigma^2 Q_{11}(t, t')$ and where

$$Q_{12}(t, t') = \langle a^t \hat{y}^{t'} \rangle = \frac{\delta \langle a^t \rangle}{\delta h^{t'}} = G(t, t') \quad (2.30)$$

$$Q_{11}(t, t') = \langle a^t a^{t'} \rangle = C(t, t'), \quad (2.31)$$

are, respectively, the response function and the correlation function of the process itself.

2.3.3 The stationary state (at fixed α)

It is possible to analyze the stationary state solution of the representative stochastic process. Since the underlying microscopic process is in fact deterministic except for its initial conditions, the stationary solution of the representative process will be a random fixed-point solution, in which the stochasticity is relegated to a quenched disorder term η^* , which represents the long-term effect of having different initial conditions. In the analysis, we also assume that, in the long-time limit, time-translation invariance holds, so that we can replace $G(t, t') = G(t - t') = G(\tau)$ and $C(t, t') = C(t - t') = C(\tau)$. At the fixed point, a^* we get the condition

$$\begin{aligned} a^* &= g\left(a^*, \alpha + \mu M^* + \sigma^2 \gamma \int d\tau G(\tau) a^* + \eta^*\right) \\ &= g\left(a^*, \alpha + \mu M^* + \sigma^2 \gamma \chi a^* + \eta^*\right) \\ &= g\left(a^*, \alpha + \mu M^* + \sigma^2 \gamma \chi a^* + \sqrt{q} \sigma \zeta\right) \end{aligned} \quad (2.32)$$

where $\eta^* = \sqrt{q} \sigma \zeta$ with $q^2 = C(0) = \langle (a^*)^2 \rangle$ and ζ is a normal random variable. The above expression gives, at fixed α ,

$$a^*(\zeta) = \max\left(0, \Theta(a^*)\left(\alpha + \mu M^* + \sigma^2 \gamma \chi a^* + \sqrt{q} \sigma \zeta\right)\right) \quad (2.33)$$

The zero solution is unstable when the argument of the function is positive, which means

$$a^*(\zeta) = \frac{\alpha + \mu M^* + \sqrt{q} \sigma \zeta}{1 - \sigma^2 \gamma \chi} \Theta\left(\frac{\alpha + \mu M^* + \sqrt{q} \sigma \zeta}{1 - \sigma^2 \gamma \chi}\right). \quad (2.34)$$

We can also compute explicit expressions for χ and q by using

$$\begin{aligned} \chi &= \frac{1}{\sqrt{q} \sigma} \left\langle \frac{\delta a^*(\zeta)}{\delta \zeta} \right\rangle_* \\ &= \frac{1}{\sqrt{q} \sigma} \int_{-\infty}^{+\infty} \frac{d\zeta}{\sqrt{2\pi}} e^{-\zeta^2/2} \frac{\delta a^*(\zeta)}{\delta \zeta}, \end{aligned}$$

$$\begin{aligned} M^* &= \langle a^*(\zeta) \rangle_* \\ &= \int_{-\infty}^{+\infty} \frac{d\zeta}{\sqrt{2\pi}} e^{-\zeta^2/2} a^*(\zeta) \end{aligned}$$

and

$$\begin{aligned} q &= \langle (a^*(\zeta))^2 \rangle_* \\ &= \int_{-\infty}^{+\infty} \frac{d\zeta}{\sqrt{2\pi}} e^{-\zeta^2/2} (a^*(\zeta))^2. \end{aligned}$$

The range $a^* > 0$ is equivalent to say that $\alpha + \mu X^* + \sqrt{q}\sigma\zeta > 0$, that is $\zeta > -\frac{\alpha + \mu M^*}{\sqrt{q}\sigma} \equiv -\Delta$; therefore, the above conditions become

$$\begin{aligned}\chi &= \frac{1}{1 - \sigma^2\gamma\chi} \int_{-\infty}^{\Delta} \frac{d\zeta}{\sqrt{2\pi}} e^{-\zeta^2/2} \\ M^* &= \frac{\sqrt{q}\sigma}{1 - \sigma^2\gamma\chi} \int_{-\infty}^{\Delta} \frac{d\zeta}{\sqrt{2\pi}} e^{-\zeta^2/2} (\Delta - \zeta) \\ 1 &= \frac{\sigma^2}{(1 - \sigma^2\gamma\chi)^2} \int_{-\infty}^{\Delta} \frac{d\zeta}{\sqrt{2\pi}} e^{-\zeta^2/2} (\Delta - \zeta)^2.\end{aligned}\tag{2.35}$$

The three equations can be solved numerically in order to find q , M^* and χ as functions of α , σ and γ .

2.3.4 Numerical procedure

To compute the order parameters as a function of σ^2 , μ and γ , the procedure is along the line of the one already seen for the GLV model. We found the same self-consistent equations, but a different definition of $\Delta = \frac{\alpha + \mu M^*}{\sqrt{q}\sigma}$. As a consequence we obtain, from the second equation of (2.35):

$$\begin{aligned}\frac{1}{M^*} &= \frac{1}{\alpha} \left(\frac{\Delta}{w_1} b - \mu \right) \\ &= \frac{1}{\alpha} \left(\frac{\Delta}{w_1} \frac{w_0}{w_2 + \gamma w_0} - \mu \right)\end{aligned}$$

And again

$$q = \left(\frac{bM^*}{\sigma w_1} \right)^2$$

$$\Phi = \int_{-\infty}^{\Delta} Dz$$

With the same definitions of w_0 , w_1 and w_2 .

This gives M, q, Φ as a function of σ^2 in parametric form.

2.3.5 Stability analysis of the stationary state

It is also possible to verify the existence of an instability of the learning process analytically, by performing a stability analysis on the representative process. We can follow a standard approach by Oppen M. and Diederich S (8). We slightly perturb the stationary state by adding a small term $\delta\zeta^t$ where ζ^t is an external normal noise and also setting perturbed values for $\eta^t = \eta^* + \delta\eta_1^t$, and $a^t = a^* + \delta a_1^t$.

The evolution equation gives

$$\begin{aligned}
a^{t+1} &= a^* + \delta a_1^{t+1} \\
&= g\left(a^* + \delta a_1^{t+1}, \alpha + \mu M^* + \sigma^2 \gamma \chi (a^* + \delta a_1^t) + \eta^* + \delta \eta_1^t\right) + \delta \zeta^t \\
&= g\left(a^*, \alpha + \mu M^* + \sigma^2 \gamma \chi a^* + \eta^*\right) \\
&\quad + g'\left(a^*, \alpha + \mu M^* + \sigma^2 \gamma \chi a^* + \eta^*\right) (\sigma^2 \gamma \chi) \delta a_1^t \\
&\quad + g'\left(a^*, \alpha + \mu M^* + \sigma^2 \gamma \chi a^* + \eta^*\right) \delta \eta_1^t + \delta \zeta^t \\
&= a^* + g'\left(a^*, \alpha + \mu M^* + \sigma^2 \gamma \chi a^* + \eta^*\right) [\sigma^2 \gamma \chi \delta a_1^t + \delta \eta_1^t] + \delta \zeta^t
\end{aligned}$$

and at $O(\delta)$

$$a_1^{t+1} = g'\left(a^*, \alpha + \mu M^* + \sigma^2 \gamma \chi a^* + \eta^*\right) [\sigma^2 \gamma \chi a_1^t + \eta_1^t] + \zeta^t.$$

Consider the autocorrelation function of the perturbation $C_1(\tau) = \sum_{t=-\infty}^{+\infty} a_1^t a_1^{t+\tau}$, for linear stability to occur we expect this quantity to decay for $\tau \rightarrow +\infty$, which means we have to analyze its Fourier transform $\tilde{C}_1(\omega)$ in the limit $\omega \rightarrow 0$. Using

$$\begin{aligned}
a_1^t &= \frac{1}{2\pi} \int_0^{2\pi} \tilde{a}_1(\omega) e^{i\omega t} d\omega \\
a_1^{t+1} &= \frac{1}{2\pi} \int_0^{2\pi} \tilde{a}_1(\omega) e^{i\omega(t+1)} d\omega
\end{aligned}$$

we get

$$\tilde{a}_1(\omega) e^{i\omega} = \sigma^2 \gamma \chi \tilde{a}_1(\omega) + \tilde{\eta}_1(\omega) + \tilde{\zeta}(\omega)$$

then

$$\tilde{a}_1(\omega) = \frac{\tilde{\eta}_1(\omega) + \tilde{\zeta}(\omega)}{e^{i\omega} - \sigma^2 \gamma \chi}$$

and averaging over the process

$$\begin{aligned}
\langle |\tilde{a}_1(\omega)|^2 \rangle &= \frac{\langle |\tilde{\eta}_1(\omega)|^2 \rangle + \langle |\tilde{\zeta}(\omega)|^2 \rangle}{(e^{i\omega} - \sigma^2 \gamma \chi)(e^{-i\omega} - \sigma^2 \gamma \chi)} \\
&= \phi \frac{\sigma^2 \langle |\tilde{a}_1(\omega)|^2 \rangle + 1}{\left(1 - (e^{i\omega} + e^{-i\omega}) \sigma^2 \gamma \chi + (\sigma^2 \gamma \chi)^2\right)}
\end{aligned}$$

in which $\phi = \Pr[a^* > 0]$ takes into account that on average only a fraction of individuals reach the non-zero fixed point. Hence,

$$\langle |\tilde{a}_1(0)|^2 \rangle = \frac{\phi}{(1 - \sigma^2 \gamma \chi)^2 - \phi \sigma^2} \quad (2.36)$$

being finite implies the stability condition

$$\frac{\phi \sigma^2}{(1 - \sigma^2 \gamma \chi)^2} \leq 1. \quad (2.37)$$

Thus finding the same results obtained in (3) for the GLV model.

$$\sigma_c^2(\gamma) = \frac{2}{(1 + \gamma)^2}$$

Chapter 3

Comparison with simulations

3.1 Introduction to the method

The theoretical results found in chapter 2 can be compared with numerical simulations of the linear quadratic model, where the renormalized aggregate of actions $M = \frac{1}{N} \sum_i a_i^*$ and fraction of surviving agents ϕ are estimated by averaging over a large number of network realizations $\{z_{ij}, z_{ji}\}_{i \neq j}$. We assume that the only form of disorder comes from the coupling parameters while the initial conditions of the game are kept fixed. Starting from a network of $N = 300$ agents, the learning process in (2.25) is numerically implemented sampling an interaction matrix \mathbf{Z} according to equations (1.2) and (1.3). Simulations start with initial conditions $a_i(t=0) = 1$, $\alpha_i = \alpha = 1 \forall i \in I$, fixing thresholds in the total number of iteration time steps, actions and M to identify the nature of the simulations. Notice that one can equivalently assume initial conditions on beliefs $\{b_i(t=0)\}_{i \in I}$ rather than actions. Different scenarios can arise as outcome of learning: a convergent Self Confirming equilibrium state where a fixed point for the conjectural best response is reached, unstable states where actions fluctuate in time, and divergent states where the aggregate of actions explodes. Although DMFT results for linear stability are equivalent to the ones found for the Generalized Lotka Volterra equations, the two models differ both in the nature of time (discrete in LQ, continuous in GLV) and in the properties of the learning process itself. The Linear Quadratic model presents a crucial non-linearity (given by the max function) which is not present in Lotka Volterra dynamics.

$$b_i^{t+1} = \begin{cases} b_i^t & \text{if } a_i^t = 0 \\ \sum_{j \in I} z_{ij} a_j^t & \text{if } a_i^t > 0 \end{cases}$$

$$a_i^{t+1} = \max \left\{ 0, \alpha + b_i^{t+1} \right\}$$

$$= \max \left\{ 0, \Theta(a_i^t) \left[\alpha + \sum_{j \in I} z_{ij} a_j^t \right] \right\}$$

While in Lotka Volterra the steady state is reached smoothly, in the LQ model the max function can change abruptly players' action depending on the competitive effect between the individual pleasure of being active α and the effect of neighbors' externalities $\sum_{j \in I} z_{ij} a_j$.

As soon as the local externalities term is sufficiently negative to guarantee the condition $\alpha + b_i^t < 0$ at a time t , agent i enters the absorbing inactive state, while in

Lotka Volterra species reach extinction smoothly. As a consequence, both M and ϕ will change abruptly during the dynamics, especially during the first iteration steps of learning. In light of this, the results on the steady state of representative agent cannot hold since it is assumed a smooth behaviour of the dynamics. To overcome this effect of non-linearity, we assume an experience weighted learning process: the action a_i^{t+1} of player i at time $t + 1$ will be a convex combination between the action at previous time step a_i^t and the upgrade due to the conjectural best response, weighted by a learning rate $\epsilon \in [0, 1]$.

$$a_i^{t+1} = (1 - \epsilon)a_i^t + \epsilon \max \left\{ 0, \Theta(a_i^t) \left[\alpha + \sum_{j \in I} z_{ij} a_j^t \right] \right\} \quad (3.1)$$

When $\epsilon = 1$, the learning in eq (2.25) is restored. The effect of the max function strictly depends on how large is the term $\sum_{j \in I} z_{ij} a_j^t$, and as consequence on the variance σ^2 of the coupling parameters: the bigger the value of σ^2 involved, the smaller the value of learning rate ϵ is needed to guarantee a smooth behaviour. When σ^2 is large, or when μ is negative and large in absolute value, negative externalities will win over the individual effort thus favouring the abrupt extinction of species through the max function. The chosen value of ϵ will be reported along with the results. Numerical simulations will be compared with the theoretical plots in Figure 3, focusing on the regime where linear stability results hold. Starting from initial conditions $a_i^0 = 1$ and $\alpha = 1$, players' action are upgraded at each time step according to eq (3.1) up until a maximum of \bar{t} time steps. Within the total time \bar{t} , simulations are either classified as convergent, unstable or divergent. The detection of a steady state is based on a threshold in the change of each player's action: in our convention a simulation reach convergence whenever the condition $|a_i^{t+1} - a_i^t| < \Delta a_{th} = 0.001$ holds $\forall i \in I$. Species are considered as survived based on a threshold in the population density at the steady state $a_i^* > \theta_{th} = 0.01$. N_s indicates the total number of surviving agents. As a consequence, for each convergent simulation $M = \frac{1}{N} \sum_i a_i^*$ and $\phi = \frac{N_s}{N}$ are computed, then their average is computed over T different realization of the network. Simulations are classified as divergent whenever the condition $M(t) \geq M_{th} = 10^3$ holds. The threshold M_{th} was chosen two orders of magnitude bigger than the theoretical results. It needs to be sufficiently bigger than the order of magnitude of convergent simulations in order to be consistent with numerical results. Finally, unstable fluctuating states are detected using the total time $\bar{t} = 10000$ as threshold: simulations that do not converge within \bar{t} are classified as unstable, the value of \bar{t} must be chosen sufficiently bigger with respect to the typical time of convergence of numerical results. First, the complete graph will be discussed in comparison with the DMFT result, also looking at the particular case of $\mu = 0$. Secondly, a purely numerical work was performed for the case of the K-Regular graph focusing on the role of the coordination number K in the stability properties of the steady state.

3.2 Case of complete graph

The results obtained in chapter 2 with dynamical field theory hold, in both models, in the case of a complete graph, where each of the N nodes in the network is connected to the rest of the community with a direct link weighted by an entry of the interaction matrix \mathbf{Z} . A crucial assumption within the theory is the thermodynamical limit $N \rightarrow \infty$, while numerical simulations are inevitably affected by finite size effects. First, a numerical example to show what is the typical behaviour of simulations for a negative value of the mean, where the stability results hold, reporting histograms and box plots for the case of $\mu = -2$, $\gamma = 1$ and a value of variance $\sigma^2 = 0.45$ near the critical one (0.5).

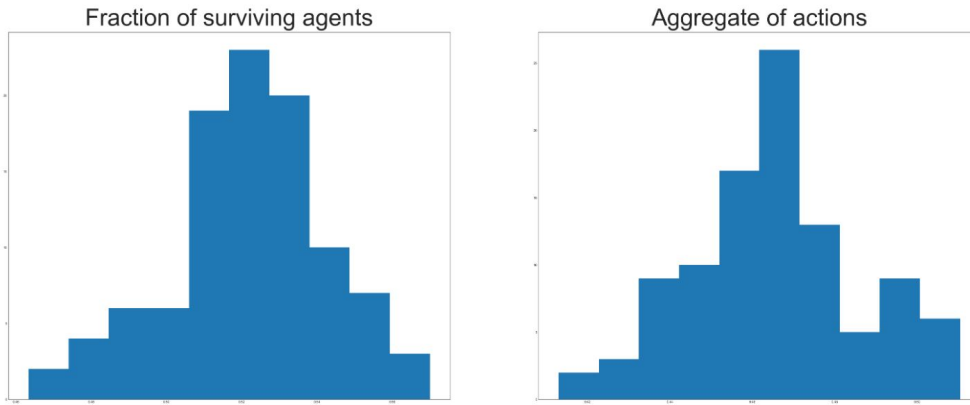


Figure 4: Histograms of ϕ , M for $\gamma = 0$, $\sigma^2 = 0.45$, $\epsilon = 0.5$

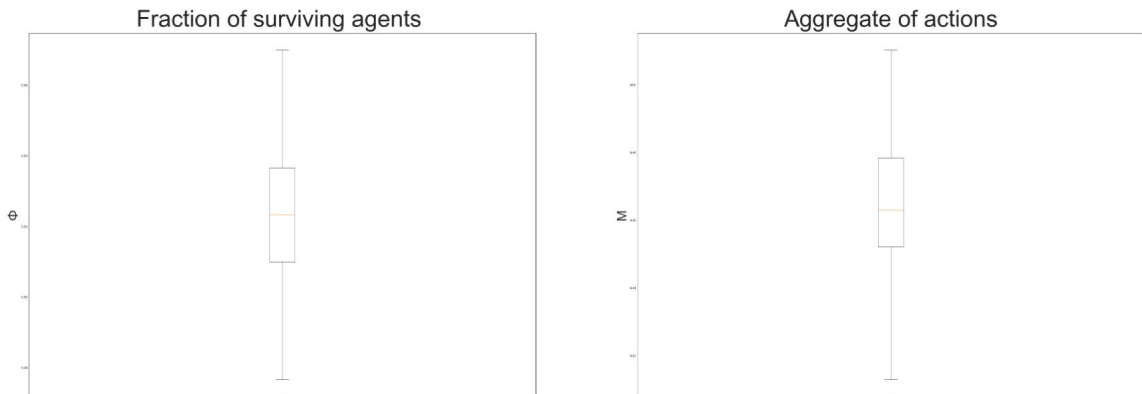


Figure 5: Box Plots of ϕ , M for $\gamma = 0$, $\sigma^2 = 0.45$, $\epsilon = 0.5$. The box plot extends from the first quartile to the third quartile of the data, with a line at the median. The whiskers extend from the box to the farthest data point lying within 1.5x of the inter-quartile range.

The results for both M and ϕ are distributed around the predicted results, with a variability that increases with the variance. Due to the finite size of the sample, the two distributions do not always behave in a gaussian like manner as one would expect in theory. As consequence, the observed results are represented by box plots instead of the mean, in order to better describe the behaviour of the bulk of simulations and the presence of possible outliers. To compare our result with the theoretical ones displayed in figure 3, for a given value γ a point (M, σ^2) and (ϕ, σ^2) will correspond to a numerical box plot of the type shown in figure 4 and 5. First,

the results are reported for $\mu = -2$ and values of $\gamma = -1, 0, 1$ with a corresponding suitable learning rate ϵ . We considered samples of 300 simulations of systems with $N = 300$ agents and $t_{th} = 2000$.

Uncorrelated interactions: $\gamma = 0$

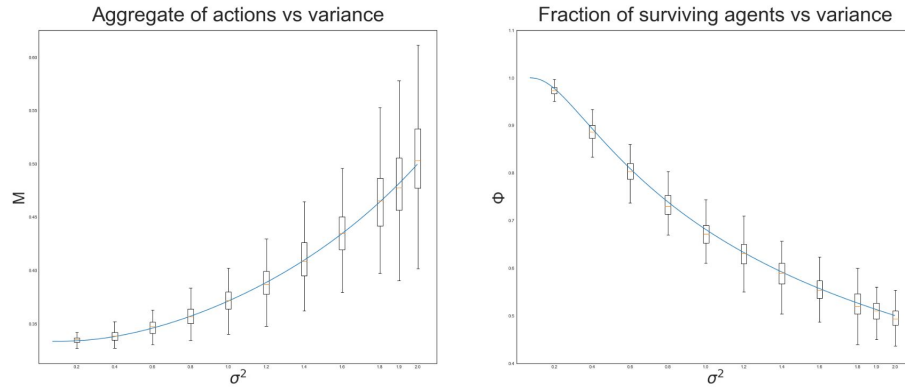


Figure 6: Numerical results for $\mu = -2$ and $\gamma = 0$, with $\epsilon = 0.5$

Correlated interactions: $\gamma = 1$

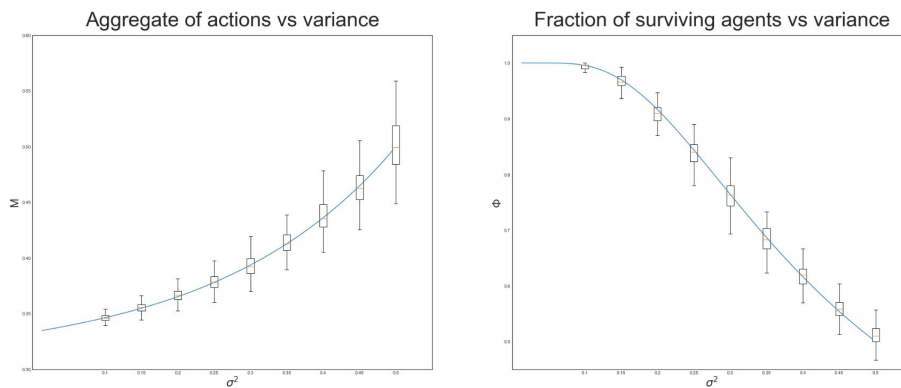


Figure 7: Numerical results for $\mu = -2$ and $\gamma = 1$, with $\epsilon = 0.5$

Anticorrelated interactions: $\gamma = -1$

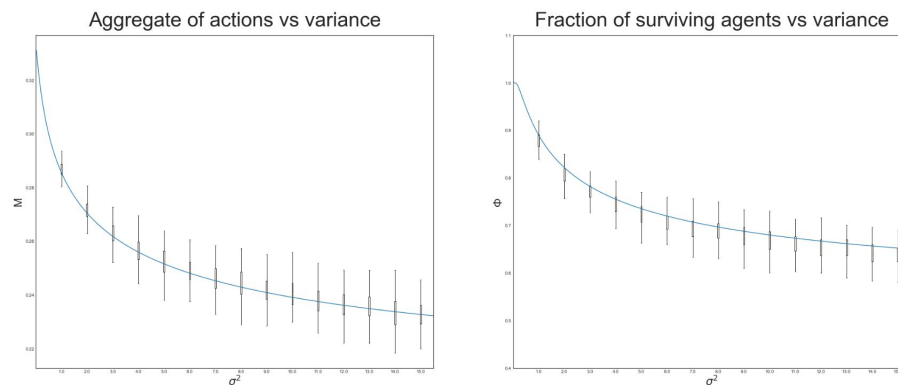


Figure 8: Numerical results for $\mu = -2$ and $\gamma = -1$, with $\epsilon = 0.05$

3.2.1 Interpretation of the results

For all cases of γ numerical results show consistency with the results found in chapter 2. In all three case the chosen value of σ^2 has a visible effect on the distribution of the renormalized aggregate of the actions M , a larger variance leads to a larger variability in the outcome of the simulations, while still being distributed around the predicted value. The same observation holds for the fraction of surviving agents ϕ . The anticorrelated case is, in the DMFT result, stable for any finite value of σ^2 , as a consequence, the value of the learning rate ϵ plays also a role in establishing a range of variance within the finite size results agree with the theory. Results show good agreement in the range $\sigma^2 \in [0, 16]$, both in M and ϕ . Decreasing further the learning rate ϵ would enlarge the possible value of σ^2 to test against the theory. On the other hand, for the case of uncorrelated and correlated interactions, decreasing further the value of ϵ has no effect on the range of stability, above the critical threshold σ_c^2 a non negligible fraction of diverging simulations is found, even in the limit of small learning rate.

3.2.2 Effect of divergence and instability

A numerical study is also reported for $\mu = 0$ and values of $\gamma = -1, 0, 1$, with a corresponding suitable learning rate ϵ . We considered samples of 300 simulations of systems with $N = 300$ agents and $t_{th} = 10000$. For this particular value of μ , if we assume that the bulk of simulations still behaves according to the predicted results, the box plot representation is more suited to show the variability of the simulations since multiple equilibrium points appear due to the emergence of instability, near the transition a variety of possible scenarios are observed, especially in the values of M^* . To show this, we look at a numerical example for the uncorrelated case $\gamma = 0$ and $\mu = 0$, for a value of the variance $\sigma^2 = 1.8$ near the critical one, with learning rate $\epsilon = 0.8$.

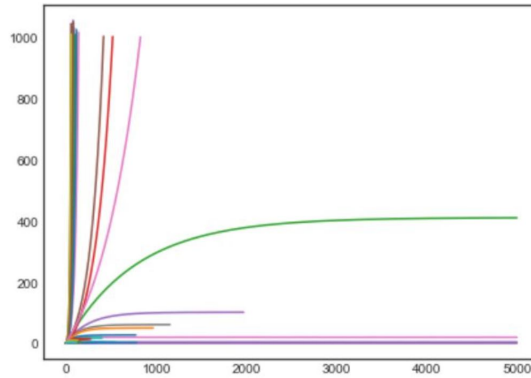


Figure 9: Dynamics of 100 simulations for M^* , with a time threshold $t_{th} = 5000$.

$\mu = 0$ is a limiting case where the critical value of variance signs the emergence of both instability and unbounded growth. In the plot of Figure 9 we find a portion of simulations that are well behaved, reaching a value M of the same order of the theoretical one (which, in this case, is roughly $M_{th} \approx 6,6$) in less than a few hundreds of steps. In other cases convergence is obtained for much higher values of M and in a much longer time (less than 2000 or more). Different steady states sign the emergence of instability, since they show the presence of history dependent

systems. Finally we also find fluctuating states with M again of the order of the theoretical one, and a variety of divergent simulations. We can look now at the distribution of M , ϕ , and total time steps for those simulations that have been classified as convergent.

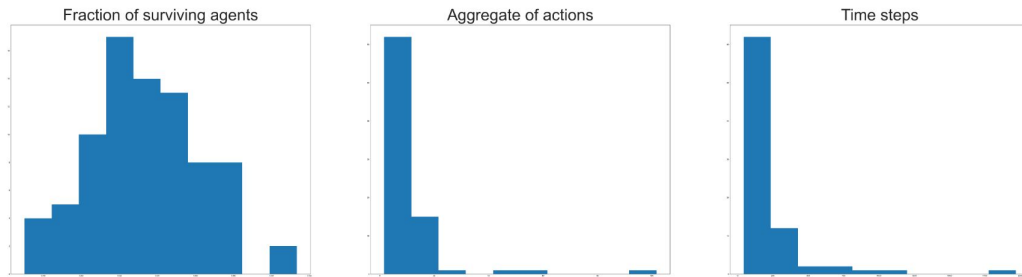


Figure 10: Histograms of ϕ , M , and time of convergence

Although the aggregate of actions does not match the expected behaviour, we assume that the bulk of simulations will still behave according to the theoretical prediction, this is the reason why we decided to describe M , ϕ and t with the median instead of the mean to capture the behaviour of the largest portion of the simulated systems. This statistical parameter also allows to capture how strong is the effect of instability, while still well representing the mean when both M and ϕ behave in a gaussian manner, like in the case of smaller variance, or more in general simulations with negative mean $\mu < 0$.



Figure 11: Corresponding box plots

First, we consider the case of correlated interactions $\gamma = 1$ and uncorrelated interactions $\gamma = 0$.

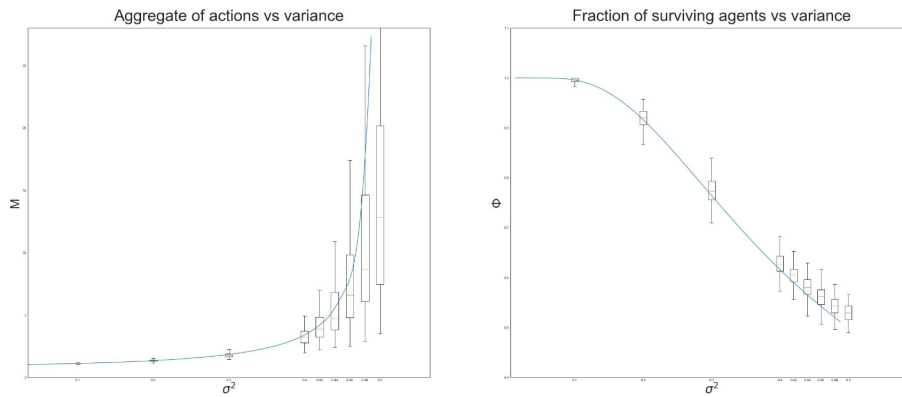


Figure 12: Numerical results for $\gamma = 1$ and $\epsilon = 0.1$

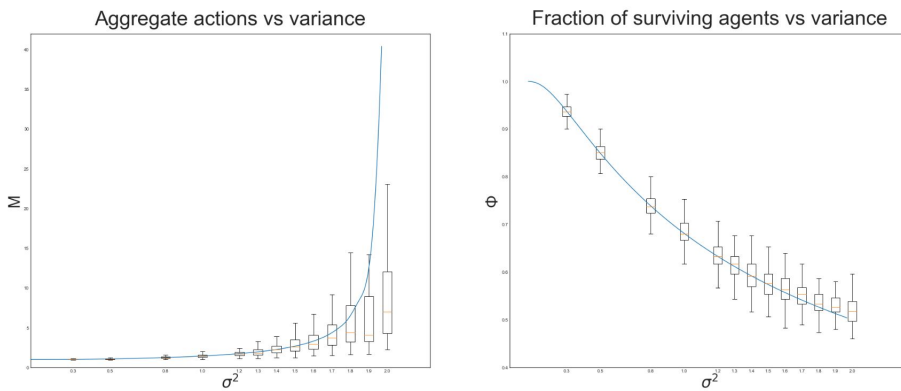


Figure 13: Numerical results for $\gamma = 0$ and $\epsilon = 0.1$

The two cases show a similar behaviour both in terms of M and ϕ . For low variances the aggregate of actions shows good agreement with the DMFT result, since the bulk of data is highly peaked around the theoretical value. The variability in M (described by the interquartile range) increases with the variance σ^2 , as well as the number of unstable simulations, either unbounded or fluctuating, and outliers of the distribution of the finite values observed. On the other hand, the fraction of surviving agents is less affected by finite size effects, showing a good agreement in both cases and even for larger variability in the interactions. The behaviour for the time of convergence follows qualitatively the one of M^* , also justifying a posteriori our choice on the chosen time threshold.

We look now at the numerical results for the anticorrelated case $\gamma = 0$.

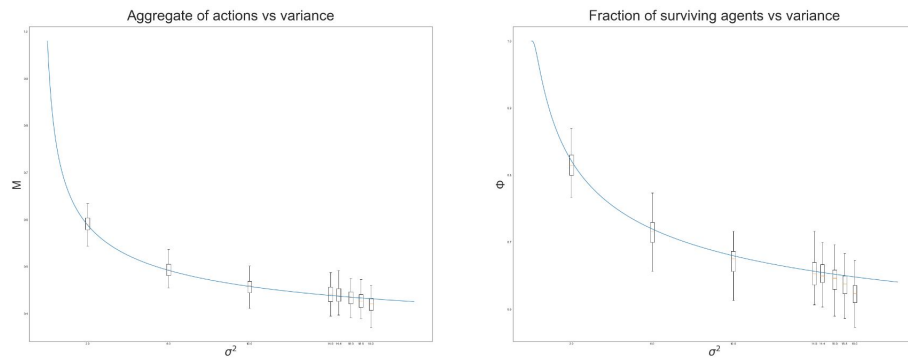


Figure 14: Numerical results for $\gamma = -1$ and $\epsilon = 0.05$

Convergent simulations are concentrated within a narrow IQR around the analytical predictions, while fluctuating simulations play the same role of the previous cases, increasing in number with the variability of couplings $\{z_{ij}, z_{ji}\}_{i \neq j}$. On the other hand, unbounded growth of M^* is never observed, coherently with what found in theory.

3.3 Case of K regular random graph

In the particular case of $\mu = 0$, numerical results show the emergence of instability before the critical threshold of variance predicted by the theory: a non negligible increasing fraction of unstable and diverging simulations is observed as the variability of interactions increases, even within the range of σ^2 where the system is, in theory, linearly stable.

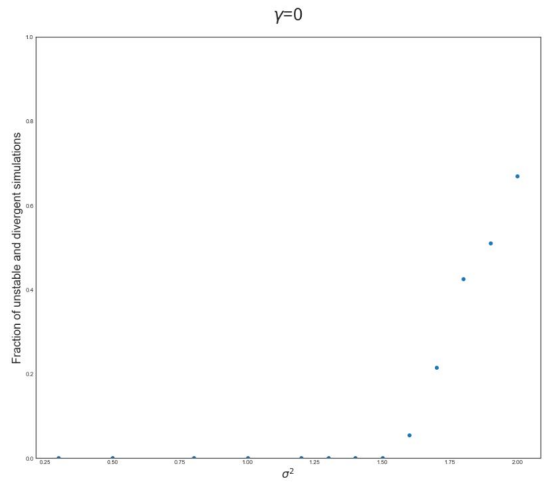


Figure 15: Fraction of unstable and diverging simulations as a function of variance σ^2 .

Numerical results for $\mu=0$, $\gamma = 0$ and $\epsilon = 0.8$

Figure 15 shows that a non negligible percentage is found as the variance increases, and the same has been observed for the other values γ . One possible explanation for this behaviour is the effect of the finite size of the system, a finite size scaling analysis is difficult to approach for this model due to the dependence of the outcomes of the dynamics not only on the system size N , but also on other parameters such as γ , σ^2 and learning rate ϵ . Nonetheless, we can explore what is the role of connectivity in determining the features of this effect. Since the DMFT results holds at the thermodynamical limit $N \rightarrow \infty$ in the complete case, where the coordination number of the network K is such that $K = N - 1$, we can already imagine that the low connectivity regime will lead to different results, that may influence the stability properties of the steady states. To qualitatively show this, we can exploit the observation that the fraction of unstable simulations increases with the variance: chosen the percentage obtained at the critical value $\sigma_c^2(\gamma)$ as threshold, we can compare what we found in the complete case with what is observed in a random K -regular graph while varying K . If the connectivity has a role in promoting stability, we expect to obtain the same percentage for higher value of variance as the connectivity increases, while matching the results for the complete graph as $K = N - 1$. Fixing $\mu = 0$, for each value of γ we performed simulations for a K -regular random graph with the same scheme used for the complete case. For each K , a critical value of variance $\sigma_{K,c}^2(\gamma)$ is identified as the smallest value for which an equal or bigger fraction of unstable and diverging simulation is observed with respect to the complete case $\sigma_c^2(\gamma)$. The plots will be reported by renormalizing the range of stability for the variance in an interval $[0, 1]$.

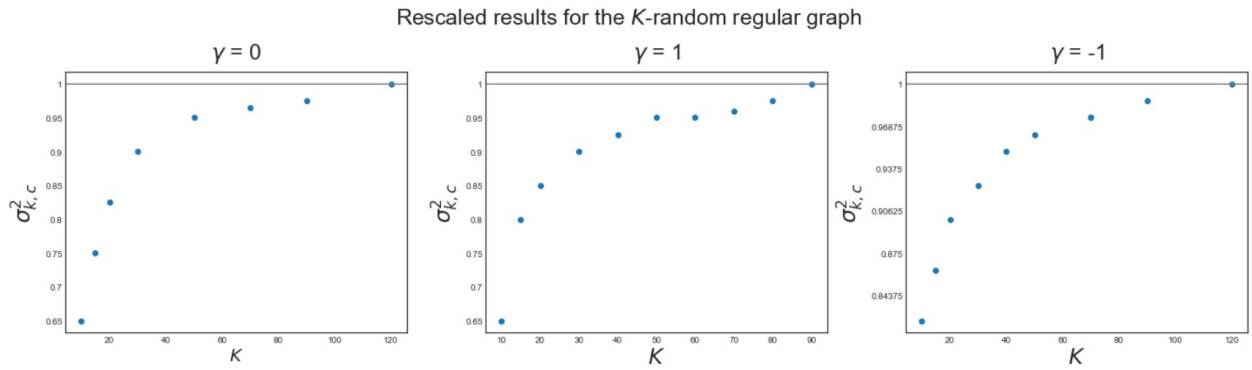


Figure 16: Results obtained for the K -random regular case for different values of γ . Gray lines represent the value of critical variance σ_c^2 obtained in the complete case.

By the results of numerical simulations connectivity seems to play a role in promoting the stability of the steady states. For small values of K systems are typically stable only within a small range of variability, in this regime the DMFT results are especially affected by the sparsity of connections. For larger values of connectivity stability is promoted, until the results of the complete graph is reached above a sufficiently large value of K (around 30% of the system size $N = 300$), after which the theoretical results for the complete case are again obtained.

Chapter 4

Conclusions

Although the Lotka Volterra and Linear Quadratic model are used in apparently different scenarios, they both investigate the role of competition and cooperation in determining the equilibrium properties of an interacting community. The learning dynamics that we applied can be imagined to represent a toy model to analyze the effect of interactions on the level of participation that agents have in an active network, where partial knowledge about the community properties affect the way an agent participate in an equilibrium state. A key assumption used to apply method is that a form of correlation exists only between pairs of interactions, which must be taken into account when applying this results to practical scenarios. Within the model, anti-correlated interactions between agents promote stability, while the variability of interactions yields the opposite effect, it reduces the size of the remaining active community, while increasing the aggregate of actions played at the steady state. Communities with larger size thus seem more likely to be stable. The DMFT results holds in a case of a complete graph, where center limit theorem arguments can be exploited in the large size limit to obtain a mean field result. Connectivity helps to stabilize the system against an increasing diversity of network interactions. As connectivity increases the typical community converge for a larger range of variability, while reaching the results of the complete case for a sufficiently connected network.

Bibliography

- (1) Ballester, C., Calvò-Armengol, A., and Zenou, Y. (2006). Who's who in networks. Wanted: the key player. *Econometrica*, Vol. 74, No. 5 (2006), 1403–1417.
- (2) Fudenberg, D., and Levine, D. K., *The Theory of Learning in Games*; The MIT press: 1998.
- (3) Galla, T. (2018). Dynamically evolved community size and stability of random Lotka-Volterra ecosystems. *EPL*, Vol 13, 48004.
- (4) M., M. R. (1973). Stability and Complexity in Model Ecosystems. *Monogr. Popul. Biol.* - 235.
- (5) Mezard M., P. G., and M., V., *Spin Glass Theory and Beyond*; World Scientific: 1993.
- (6) Battigalli, P., Panebianco, F., and Pin, P. (2022). Learning and Selfconfirming Equilibria in Network Games.
- (7) Bunin, G. (2017). Ecological communities with Lotka-Volterra dynamics. *Phys. Rev. E* 95, 042414.
- (8) M., O., and S., D. (1992). Phase transition and $1/f$ noise in a game dynamical model. *Phys. Rev. Lett.* 69, 1616.